



T-279

Volume I

**ERRORS OF A LINEAR INTEGRATING
ACCELEROMETER UNDER A
VIBRATION ENVIRONMENT**

by

Julius Feldman

B. M. E. , City College of New York, 1954

**Submitted in Partial Fulfillment
of the Requirements for the
Degree of Master of Science
at the
MASSACHUSETTS INSTITUTE OF TECHNOLOGY
May 1961**

Signature of Author _____
**Department of Aeronautics and
Astronautics, May 1961**

Certified by _____
Thesis Supervisor

Accepted by _____
**Chairman, Departmental Committee
on Graduate Students**

**ERRORS OF A LINEAR INTEGRATING ACCELEROMETER
UNDER A VIBRATION ENVIRONMENT**

by

Julius Feldman

Submitted to the Department of Aeronautics and Astronautics
on May 19, 1961, in partial fulfillment of the requirement for the
degree of Master of Science.

ABSTRACT

Studies have been conducted to determine the errors in the accelerations indicated by a pendulous integrating gyro accelerometer due to various dynamic environments.

Errors in measured acceleration caused by combinations of steady-state and vibratory translational accelerations are obtained.

The acceleration errors resulting from misalignment between the LIX gyro input and control-member axes and when the LIX unit is subjected to angular vibration are also obtained.

The loop dynamics for the LIX unit is presented. A change in the loop to minimize the acceleration errors is suggested.

Thesis Supervisor: R. K. Mueller

**Title: Associate Professor of
Aeronautics and Astronautics**

ACKNOWLEDGEMENTS

The author wishes to express his sincere appreciation to the many persons in the Instrumentation Laboratory of the Massachusetts Institute of Technology whose cooperation and assistance made this thesis possible. He is particularly indebted to:

Professor R. K. Mueller, Associate Professor of Aeronautics and Astronautics for his guidance as thesis supervisor.

Messrs. P. J. Palmer and W. A. Gianoukos for their interest and encouragement in the work.

Messrs. A. J. Smith and H. Weinstock who inspired and guided the entire project as technical advisers.

Miss Irene M. Ezer for her patience and skill in typing the manuscript.

Mrs. K. Sylva for her assistance in preliminary typing.

Mr. M. Perkins for his assistance with plotting and drawing; and to Mr. E. J. Carbrey of Jackson and Moreland for his advice and assistance in the publishing of this thesis.

This thesis was prepared under the auspices of DSR project 52-155 sponsored by the Weapons Guidance Laboratory of Wright Air Development Center through USAF Contract AF 33(616)-6070.

14

Publication of this document does not imply approval of, or agreement with, any of its findings or conclusions by either the United States Air Force or MIT Instrumentation Laboratory. It is published only to promote the exchange and stimulation of ideas.

TABLE OF CONTENTS

<u>Chapter</u>	<u>Title</u>	<u>Page</u>
1	Introduction	1
2	Construction and Theory of Operation of the Linear Integrating Accelerometer	2
2.1	Construction	2
2.2	Theory of Operation	6
3	Pendulum Unit used as Acceleration Measuring Devices	10
3.1	Introduction	10
3.2	Pendulum with Damping and Restraint Subjected to a Linear Acceleration at an Angle to the Pendulum Sensitive Axis	10
3.3	Pendulum with Damping and Restraint Subjected to a Linear Vibration along the Pendulum Sensitive Axis	13
3.4	Pendulum with Restraint and Damping Subjected to a Linear Vibration at an Angle to Pendulum Sensitive Axis	15
4	Cross-Couling and Vibropendulum LIX Errors Obtained for Small Rotation of the Control- Member Axis	21
4.1	Introduction	21
4.2	Equation of Motion of LIX Subjected to a Translational Acceleration	21
4.3	Control-Member Performance Function, A Constant	24
4.4	Control-Member Performance Function, An Integrator	27

TABLE OF CONTENTS (cont.)

<u>Chapter</u>	<u>Title</u>	<u>Page</u>
5	Cross-Coupling, Vibropendulum, and Misalignment LIX Errors Averaged Over a Period of Control-Member Rotation	32
5.1	Introduction.	32
5.2	Cross-Coupling Error for Condition of Perfect Unit Alignment	33
5.3	Cross-Coupling Error Due to Misalignment Between LIX Gyro Input and Control-Member Axes	38
5.4	Vibropendulum Error for LIX Unit Subjected to Vibration at an Angle to the Control-Member Axis	41
5.5	Vibropendulum Error for Vibration Applied at an Angle to Control-Member Axis while a Constant Acceleration is being Applied Along LIX Input Axis	45
5.6	Vibropendulum Error for Misalignment between LIX Gyro Input and Control-Member Axes	48
6	Errors due to Angular Vibration About Two Axes in the Plane of the LIX Gyro Spin and Output Axes	53
6.1	Introduction.	53
6.2	Definitions and Symbols	55
6.3	Component of Angular Vibration about the LIX Gyro Output and Spin Reference Axes as the Control Member Rotates. . . .	58
6.4	Coning Error When the Performance Function of the Control-Member Drive is a Constant Gain.	59
6.5	Coning Error When the Performance Function of the Control-Member Drive is an Integrator	66

TABLE OF CONTENTS (cont.)

<u>Chapter</u>	<u>Title</u>	<u>Page</u>
7	LIX Loop Dynamics	71
7.1	Introduction	71
7.2	Performance Function of an Ideal Pendulous Integrating Gyro Unit.	71
7.3	Performance Function of LIX Drive Motor	73
7.4	Performance Function of LIX Unit.	75
7.5	Control-Member Drive Performance Function with an Integrator	80
8	Conclusions and Recommendations	82
8.1	Conclusions	82
8.2	Recommendations	83
 <u>Appendix</u>		
A	Vibropendulous and Cross-Coupling Torque for Pendulum having Elastic Restraint and Damping.	85
A.1	Equation of Motion of a Pendulum Subjected to Translational Acceleration	85
A.2	Pendulum Subjected to a Constant and Sinusoidal Acceleration at an Angle to the Pendulum Sensitive Axis	87
A.3	Pendulum Subjected to a Vibration at an Angle to the Pendulum Sensitive Axis and Rotating Acceleration Vector	94
Bibliography		100

LIST OF ILLUSTRATIONS

<u>Figure</u>	<u>Title</u>	<u>Page</u>
2-1	Line schematic of linear integrating Accelerometer LIX	5
2-2	Functional Diagram of linear integrating accelerometer	7
3-1	Pictorial schematic diagram of the single-degree-of-freedom floated pendulum specific force receiver -- Line schematic diagram for the single-degree-of-freedom floated pendulum specific force receiver	11
3-2	Restrained damped pendulum subjected to linear acceleration	12
3-3	Restrained damped pendulum subjected to linear vibration.	13
3-4	Frequency response of highly damped restrained pendulum	14
3-5	Restrained damped pendulum subjected to linear vibration.	15
3-6	Vibropendulum torque (M_{VP}) of a pendulum unit with elastic restraint (K) and damping (C) subjected to a vibration ($a \sin \omega t$) at an angle (α) to the pendulum sensitive axis	16
3-7	Simple pendulum deflection in phase with acceleration	17
3-8	Acceleration, deflection, and pendulum torque vs. time for deflection lagging acceleration by 90°	18
3-9	Acceleration, vibration, and torque vs. time for a simple pendulum whose displacement lags applied acceleration by 90°	19

LIST OF ILLUSTRATIONS (cont.)

<u>Figure</u>	<u>Title</u>	<u>Page</u>
4-1	Block diagram of LIX system	23
5-1	Modification of LIX torques with control-member rotation	34
5-2	Misalignment angles of LIX unit	39
5-3	Velocity error vs. time for LIX unit subjected to vibration input	45
6-1	Drift resulting from angular vibration about gyro spin and output axes	54
6-2	LIX unit mounted in gimbal	58
6-3	Acceleration error vs. control-member angle	65
7-1	Pendulous Integrating Gyro	72
7-2	Block diagram of pendulous integrating gyro	73
7-3	DC torque motor	73
7-4	Block diagram of linear integrating accelerometer	76
7-5	Block diagram of LIX unit	77
7-6	Block diagram of LIX unit	78
7-7	Control-member drive performance function vs. frequency ratio for typical gyro pendulum accelerometer	79
A-1	Restrained pendulum subjected to translational acceleration	86
A-2	Pendulum subjected to a constant and sinusoidal acceleration	87
A-3	Vibration at angle α to pendulum sensitive axis — Vibration produced by acceleration vector rotating about pendulum pivot	94

CHAPTER 1

INTRODUCTION

Inertial navigation and guidance systems use accelerometers to measure the acceleration of the vehicle in which they are contained. The outputs of these accelerometers are integrated to obtain signals corresponding to the velocity and position of the vehicle. Errors in the measurement of true vehicle accelerations by these accelerometers will therefore result in errors in the trajectory of the vehicle. Accelerations perpendicular to the sensitive axis of the accelerometers or combinations of translational and rotational vibrations will produce such errors in the measurement of true acceleration.

This document investigates the acceleration indicated by the linear integrating accelerometer (LIX) due to various environmental steady-state and vibratory inputs.

The linear integrating accelerometer is a pendulous integrating gyro accelerometer of the type commonly used in inertial navigation systems. It is designed and built by the Inertial Gyro Group of the Instrumentation Laboratory. A knowledge of the effect of unit parameters on these errors may provide a means for reducing their detrimental effect.

This thesis is published in two volumes. In Volume I, errors due to translational acceleration and vibration, angular vibration, and errors caused by misalignments of the unit axes are determined. This volume is unclassified, and the results apply to any pendulous integrating gyro accelerometer.

Volume II is the classified supplement to Volume I. The errors for the various vibration inputs discussed in Volume I are applied to the LIX unit in this second volume. Chapter numbering in both volumes correspond.

Previous investigators have qualitatively defined the errors of a pendulous integrating gyro accelerometer. Some of the errors are produced by translational accelerations and vibrations. The results of these investigations are reported in references 1, 2, 3, 4, and 16. These errors have been named cross-coupling and vibropendulum errors. The nature and cause of these errors are discussed for a simple pendulum restrained by a spring and a damper in Chapter 3.

In Chapter 4, under the condition of small rotation of the control-member axis, the acceleration errors of the linear integrating accelerometer subjected to a combination of translational vibration and acceleration are determined. The analysis considers two float restraints; one exerting a torque proportional to the float displacement, and one exerting a torque proportional to the integral of float displacement.

A method to find the errors in measured acceleration averaged over a revolution of the control member have been

suggested by other authors in references 3 and 4. The LIX acceleration errors produced by translational acceleration or vibration averaged over complete revolutions of the control member are presented in Chapter 5. Errors are determined for perfect alignment between the LIX gyro input and control-member axes, and for small misalignments between these axes.

Results are presented so that actual acceleration errors for any pendulous gyro accelerometer can be determined.

The drift of a single-degree-of-freedom integrating gyroscope when subjected to angular vibration has been discussed by previous investigators in references 6 and 15. This drift phenomenon is commonly called the "coning error."

In Chapter 6, the error in measurement of true acceleration when the linear integrating accelerometer is subjected to angular vibration is determined.

The control-loop dynamics of a gyro pendulum accelerometer is discussed in references 1 and 5. Chapter 7 determines the loop dynamics for the LIX accelerometer. A method of reducing the acceleration errors by adding an integrator to the control-member drive loop is also discussed.

The errors in measured acceleration when each input discussed in Volume I is applied to the LIX unit is determined in Volume II.

The results of this investigation and suggestions for future investigations are summarized in Chapter 8.

CHAPTER 2

CONSTRUCTION AND THEORY OF OPERATION OF THE LINEAR INTEGRATING ACCELEROMETER

2.1 CONSTRUCTION

A pictorial schematic of the linear integrating accelerometer (LIX) is shown in Fig. 2-1. The unit consists of a pendulous integrating gyro unit, a power-control system, a servo-drive motor, and an output angle indicator. The gyro case and servo motor are mounted in bearings (not shown in Fig. 2-1) so that the servo motor can rotate the complete gyro case about its input axis. This axis of rotation is defined as the LIX control-member axis.

The output angle indicator obtains the angular velocity and angular position of the control member shaft.

The pendulous integrating gyro unit is a single-degree-of-freedom pendulous floated gyro. The wheel and gimbal of the gyro is hermetically sealed in a cylindrical can, which is called the float. The float has a pendulosity along its spin axis. This will cause a torque about the gyro output axis when an acceleration is applied along its input axis. This assembly is floated in a viscous fluid which offers rotational damping and has the density required to provide neutral

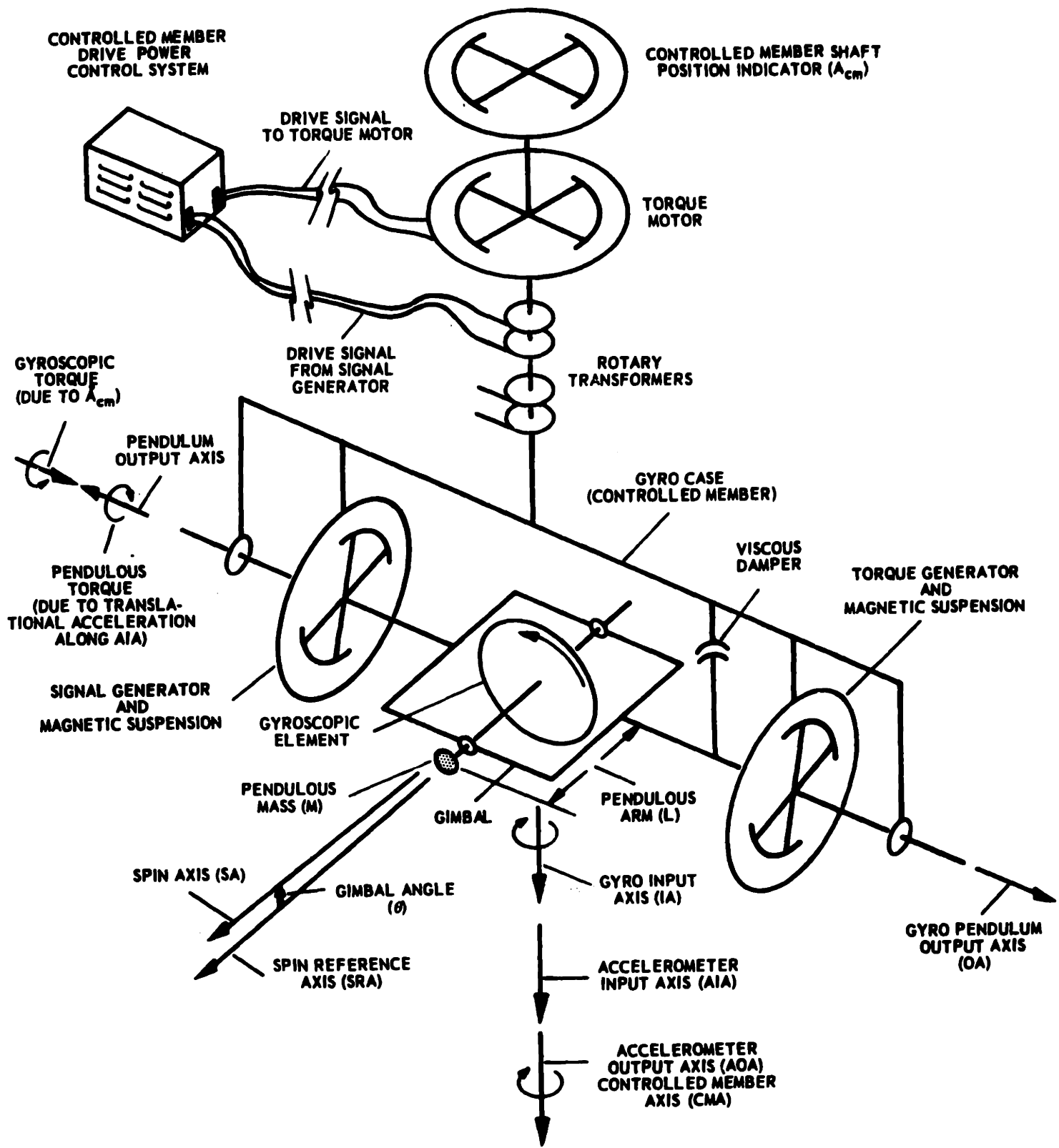


Fig. 2-1. Line schematic of linear integrating accelerometer (LIX).

buoyancy. Rotors are mounted at both ends of the float.

The rotor at one end of the float is part of a signal generator which measures float rotational position. The unit at the other end of the float is a torque generator which will torque the float when current is supplied to it. Nominal values of this gyro unit are given in reference 13. This unit is similar in construction to those discussed in detail in reference 3.

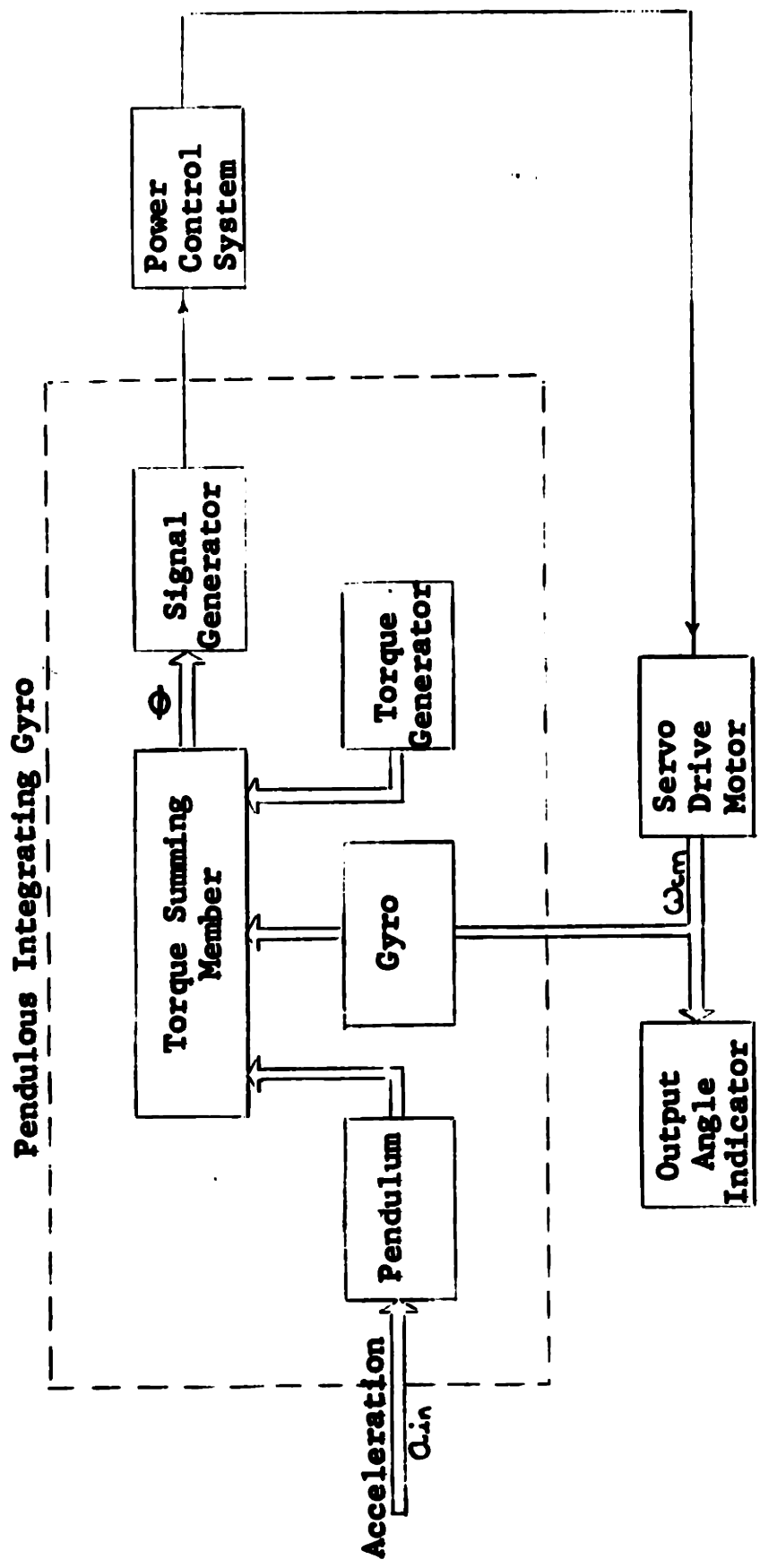
Figure 2-2 is the functional diagram for the linear integrating accelerometer. The performance function (the ratio of control-member angular velocity to input linear acceleration) for the servo loop is derived in Chapter 7.

Average unit parameters and construction information for the pendulous integrating gyro and the linear integrating accelerometer can be obtained from references 12 and 13.

The unit parameters necessary for dynamic analysis and servo-loop analysis are given in the classified supplement of this report (Volume II).

2.2 THEORY OF OPERATION

Due to the pendulosity of the gyro float, an acceleration along the accelerometer input axis will cause a torque about the gyro output axis which will attempt to rotate the gyro float through an angle. The signal from the signal generator fed through the servo loop will cause the servo motor to rotate the gyro unit about its input axis so that the acceleration-caused pendulous torque is balanced by angular velocity induced gyroscopic torque.



Functional Diagram of Linear Integrating Accelerometer
Fig 2-2

In closed-loop operation, the gyro float will be maintained at null within the loop dynamics. The gyro float is the torque summing member for the LIX unit.

The sum of the torques acting on the gyro float due to an acceleration (a_n) applied along the LIX input axis is given by

$$I\ddot{\theta} + C_d \dot{\theta} + H\omega_{cm} = mL a_n \quad (2-1)$$

where

I = moment of inertia of the gyro float about its output axis (gm-cm^2)

C_d = rotational damping coefficient of gyro float about its output axis ($\text{dyne-cm/radians/sec}$)

H = angular momentum of gyro wheel ($\text{gm-cm}^2/\text{sec}$)

ω_{cm} = angular velocity of control member (radians/sec)

mL = gyro float pendulosity along its spin axis (gm-cm)

a_n = acceleration input along the LIX input axis (cm/sec^2)

The steady-state solution of equation (2-1) is

$$\omega_{cm} = \frac{mL}{H} a_n \quad (2-2)$$

The output angle indicator is used to indicate control-member angular position (A_{cm}). The steady-state control-member angular position will be related to the linear acceleration applied along the LIX input axis by the relationship

$$A_{cm} = \left(\frac{mL}{H} \right) \int_0^t a_{in} dt \quad (2-3)$$

Equation (2-3) illustrates the integrating feature of the LIX unit. The output of the instrument, the control-member angular position (A_{cm}), is proportional to the integral of the input acceleration (a_{in}).

CHAPTER 3

PENDULUM UNIT USED AS ACCELERATION MEASURING DEVICES

3.1 INTRODUCTION

Cross-coupling and vibropendulum errors are determined for a simple pendulum having elastic restraint and damping. This analysis serves as an introduction to the analysis of the LIX unit in Chapters 4 and 5. The information of this section can be applied directly to a floated pendulous specific-force receiver (shown pictorially in Fig. 3-1) to determine the cross-coupling and vibropendulum errors due to acceleration and vibration.

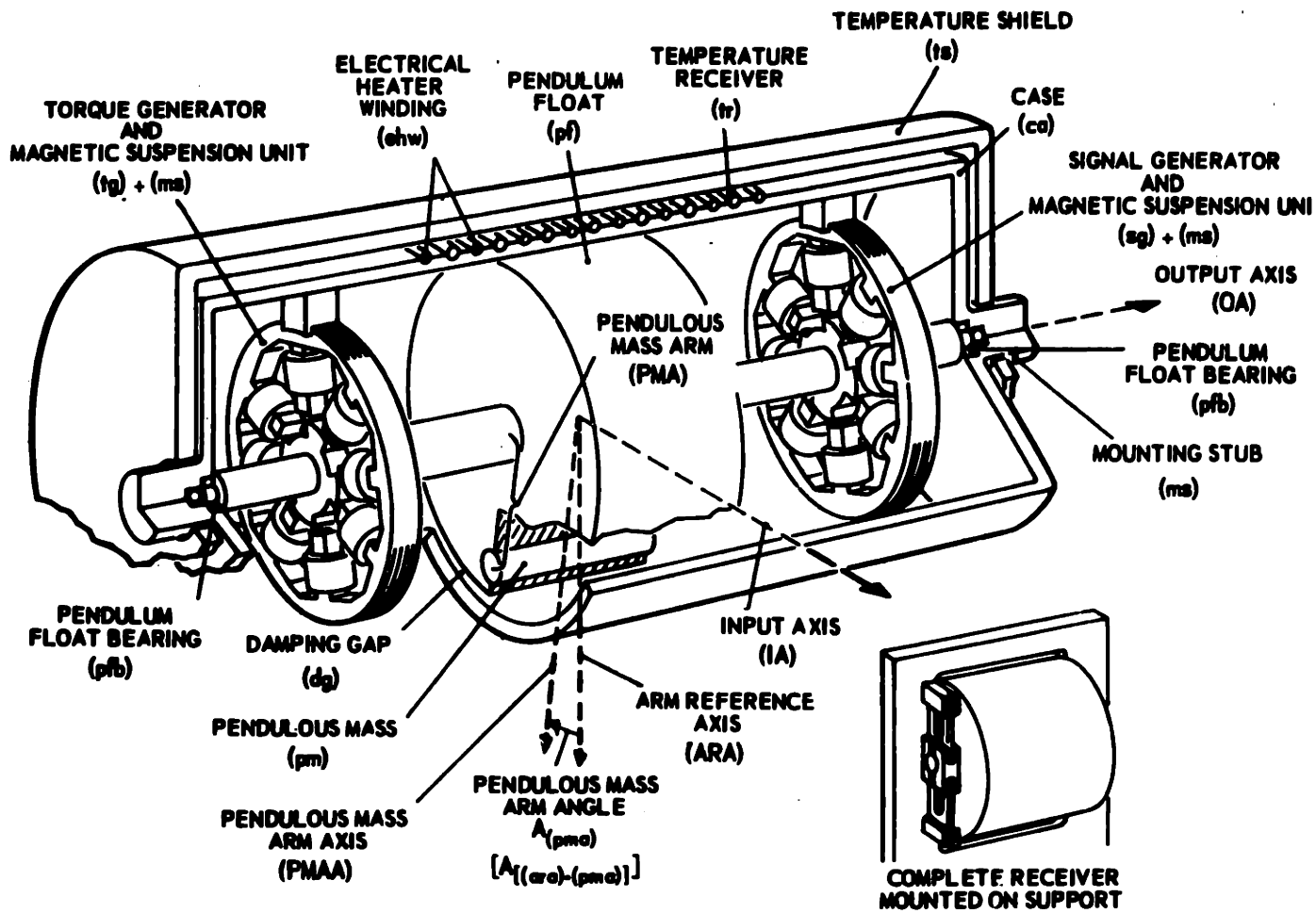
3.2 PENDULUM WITH DAMPING AND RESTRAINT SUBJECTED TO A LINEAR ACCELERATION AT AN ANGLE TO THE PENDULUM SENSITIVE AXIS

Consider the pendulum shown in Fig. 3-2 having elastic restraint and damping subjected to an acceleration a at an angle α to the pendulum sensitive axis.

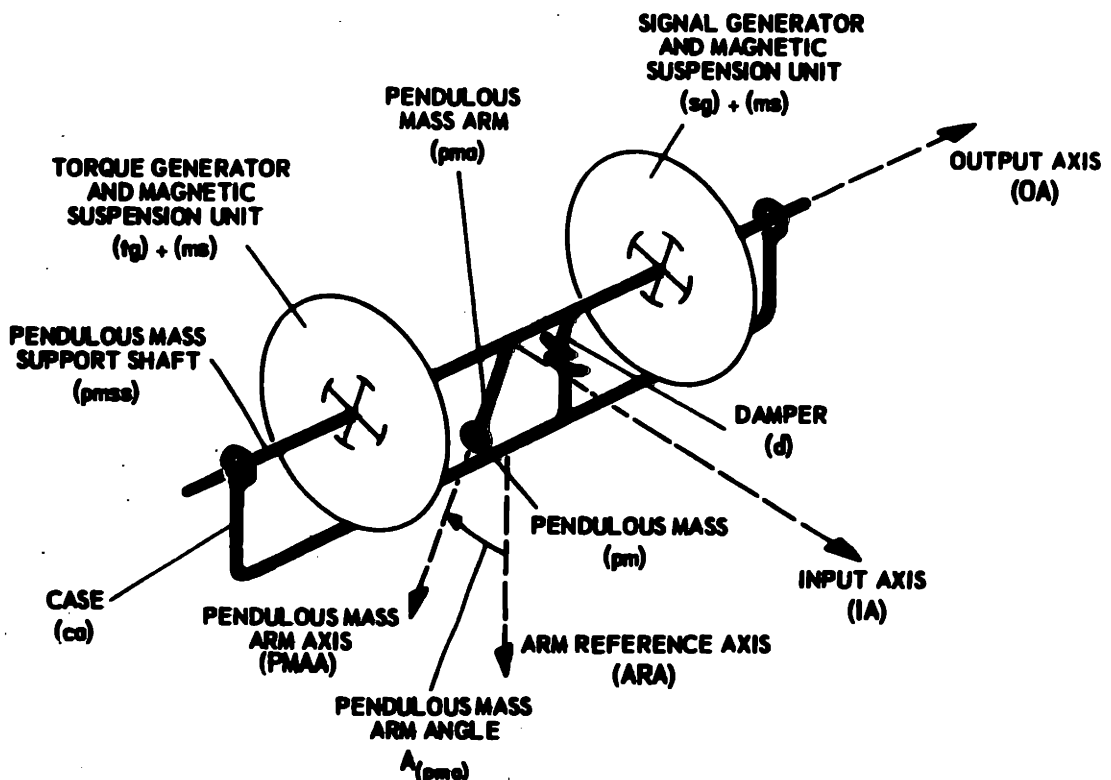
The equation of motion of the pendulum becomes (for θ small)

$$I\ddot{\theta} + C\dot{\theta} + K\theta = mL a (\cos \alpha + \theta \sin \alpha) \tag{3-1}$$

- where
- I = moment of inertia about pendulum pivot ($gm\text{-}cm^2$)
 - C = damping coefficient about pendulum pivot ($\frac{dy\text{-}cm\text{-}sec}{rad}$)
 - K = rotational stiffness about pendulum pivot ($\frac{dy\text{-}cm}{rad}$)

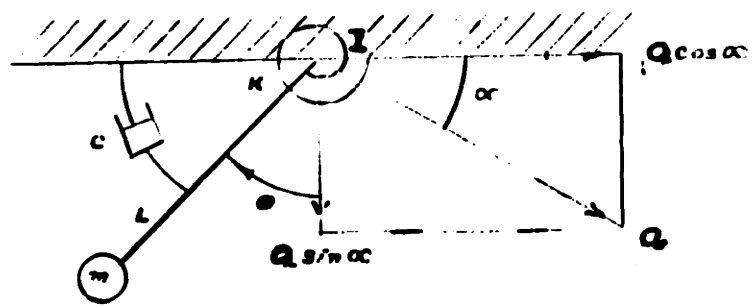


Pictorial schematic diagram of the single-degree-of-freedom floated pendulum specific force receiver.



Line schematic diagram for the single-degree-of-freedom floated pendulum specific force receiver.

- m = mass of pendulum (gm)
- L = length of pendulum arm (cm)
- θ = angle measured from pendulum position under no input acceleration to the pendulum position under the applied acceleration (radian)
- a = input acceleration (cm/sec²)
- α = angle between input acceleration and pendulum sensitive axis (degrees)



Restrained damped pendulum subjected to linear acceleration

Fig. 3-2

Equation (3-1) can be solved by an iteration procedure. Assume the pendulum deflection angle is due only to the component of acceleration along the sensitive axis. For this case, the pendulum deflection angle is

$$\theta = \frac{mLa}{K} \cos \alpha \tag{3-2}$$

Substituting the value of θ from equation (3-2) into the $(mLa \sin \alpha)\theta$ term of equation (3-1) yields

$$I\ddot{\theta} + C\dot{\theta} + K\theta = mLa \cos \alpha + \frac{(mLa)^2}{K} \cos \alpha \sin \alpha \tag{3-3}$$

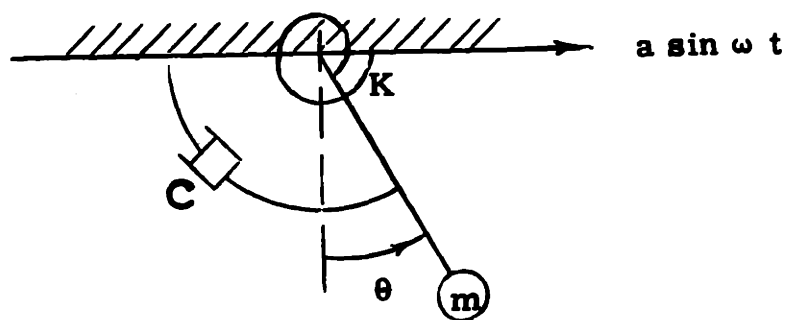
The torque due to the component of acceleration perpendicular to the pendulum sensitive axis has been named cross-coupling torque (M_{cp}) and from equation (3-3) is equal to

$$M_{(cp)} = \frac{(mLa.)^2 \sin 2\alpha}{2K} \quad (3-4)$$

From equation (3-4), the cross-coupling torque decreases with increasing elastic restraint; therefore, a high restraint must be used to keep the cross-coupling error within the accuracy requirement for the instrument.

3.3 PENDULUM WITH DAMPING AND RESTRAINT SUBJECTED TO A LINEAR VIBRATION ALONG THE PENDULUM SENSITIVE AXIS

Consider the pendulum shown in Fig. 3-3 subjected to a vibration ($a \sin \omega t$) along the pendulum sensitive axis.



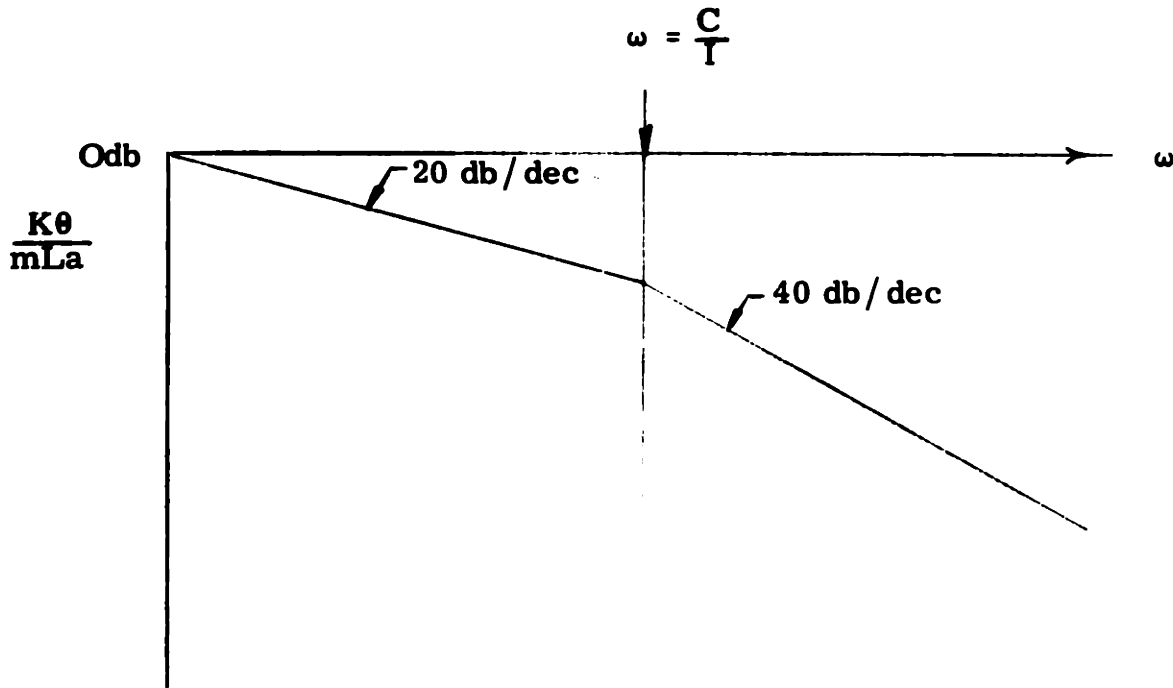
Restrained damped pendulum subjected to linear vibration

Fig. 3-3

The equation of motion of the pendulum becomes

$$I\ddot{\theta} + C\dot{\theta} + K\theta = mL a \sin \omega t \quad (3-5)$$

For pendulum accelerometers, the constants of equation (3-5) are selected so that $C \gg \sqrt{KI}$. For this case, the ratio of pendulum restraint torque to acceleration torque vs. frequency could be approximated by Fig. 3-4.



Frequency response of highly damped restrained pendulum

Fig. 3-4

The large damping will cause the pendulum bob to lag the applied acceleration for vibrational frequencies greater than zero. At very low frequencies

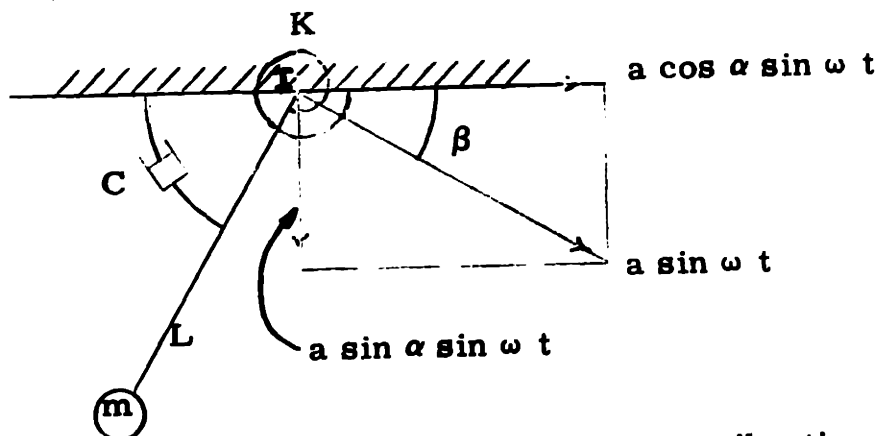
$$\theta \approx \frac{mLa}{K} \quad (3-6)$$

At higher frequencies

$$\theta \ll \frac{mLa}{K} \quad (3-7)$$

3.4 PENDULUM WITH RESTRAINT AND DAMPING SUBJECTED TO A LINEAR VIBRATION AT AN ANGLE TO PENDULUM SENSITIVE AXIS

Consider the pendulum shown in Fig. 3-5 subjected to a vibration at an angle β to the pendulum sensitive axis.



Restrained damped pendulum subjected to linear vibration
Fig. 3-5

The equation of motion of the pendulum becomes

$$I\ddot{\theta} + C\dot{\theta} + (K - mL a \sin \alpha \sin \omega t) \theta = mL a \cos \alpha \sin \omega t \quad (3-8)$$

Equation (3-8) can be solved by the perturbation method of Appendix A.

There will be an average float deflection angle and an average torque (the vibropendulum torque) over a cycle of vibration given by

$$M_{(vp)} = \frac{(mLa)^2 \sin 2\alpha (1 - \mu)}{4K \left[(1 - \mu)^2 + \mu \frac{C^2}{KI} \right]} \quad (3-9)$$

where

$$\mu = \frac{I\omega^2}{K}$$

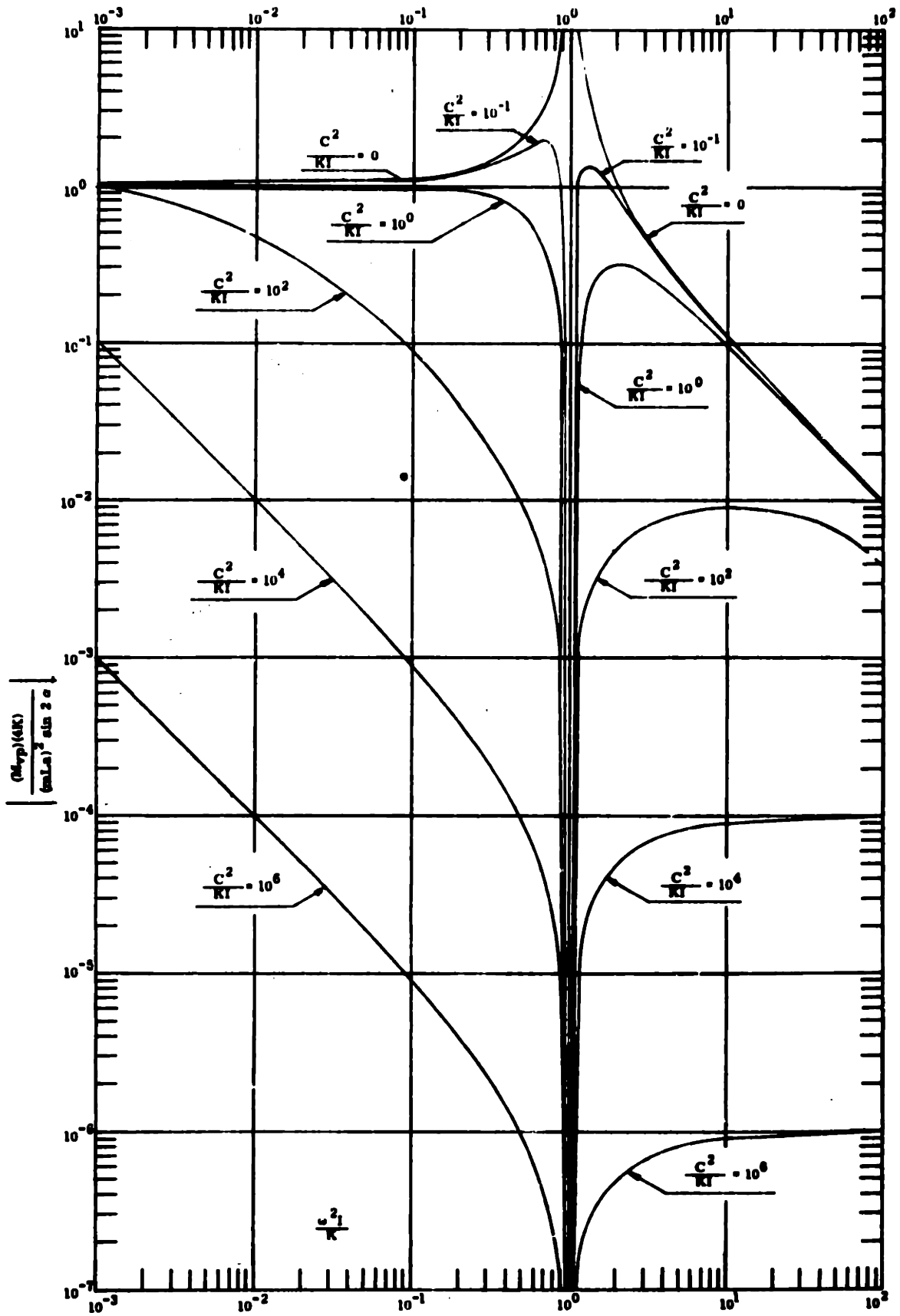


Fig. 3-6

Vibropendulum torque (M_{vp}) of a pendulum unit with an elastic restraint (K) and a damping (C) subjected to a vibration ($a \sin \omega t$) at an angle (α) to the pendulum sensitive axis.

Figure 3-6 is a plot of $\frac{M_{(vp)} 4K}{(mLa)^2 \sin 2\alpha}$ vs. $\frac{I\omega^2}{K}$ for various values of $\frac{C^2}{KI}$. From this graph, the variation of vibropendulum torque with frequency can be obtained for various pendulum parameters.

The cause of this average torque is discussed in reference 16 and is illustrated in Figs. 3-7, 3-8, and 3-9.

Consider a pendulum subjected to an acceleration \ddot{X} parallel to the pendulum sensitive axis, and an acceleration \ddot{Y} perpendicular to the pendulum sensitive axis. If the pendulum deflection is in phase with the acceleration, the pendulum at two positions of its swing is shown in Fig. 3-7.

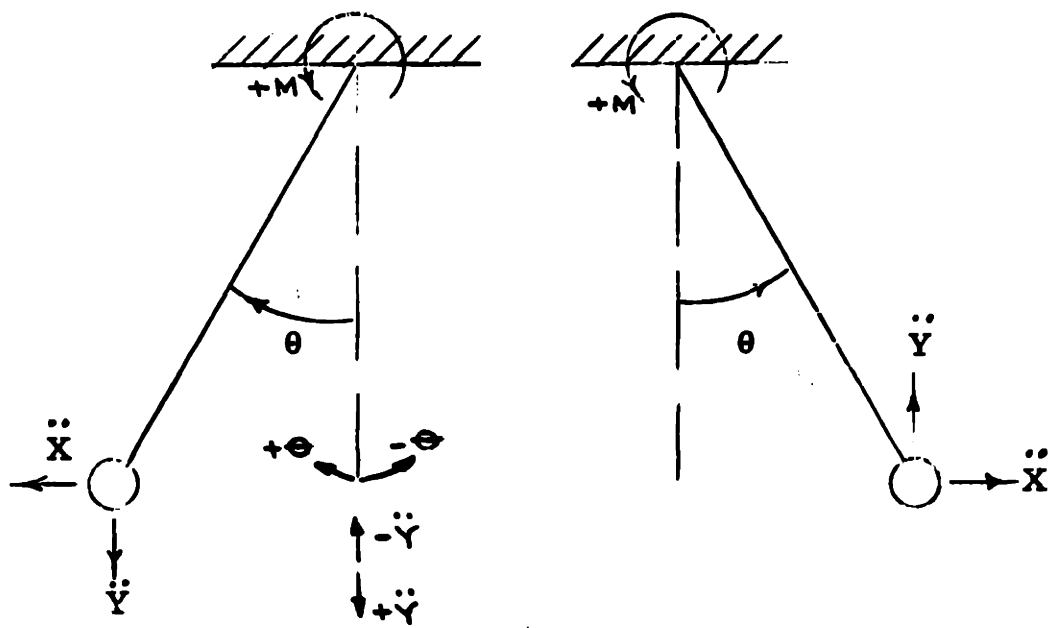
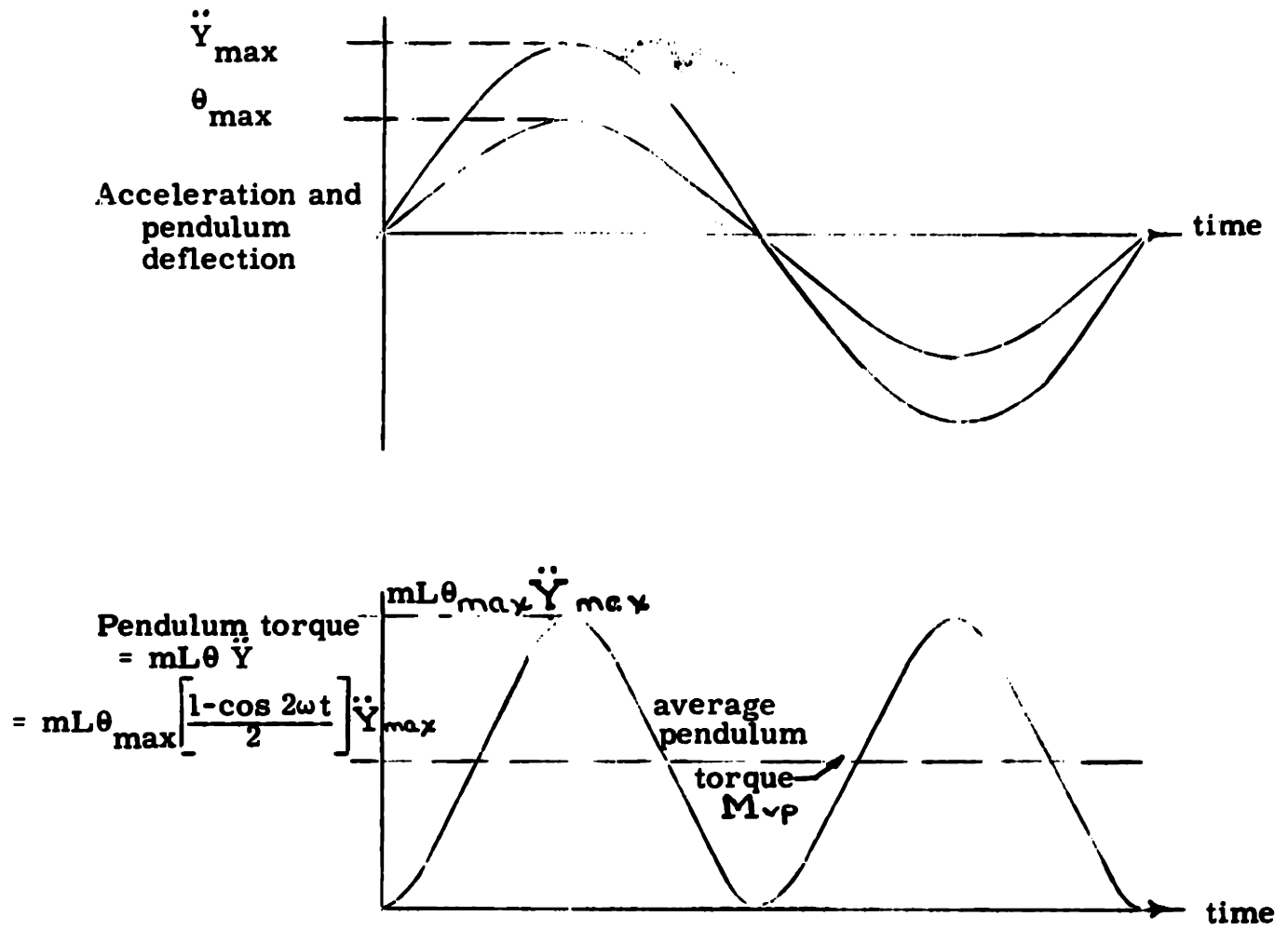


Fig. 3-7
Simple pendulum deflection in phase with acceleration

The \ddot{Y} component of acceleration, the pendulum deflection angle and torque vs. time for this case is illustrated in Fig. 3-8.



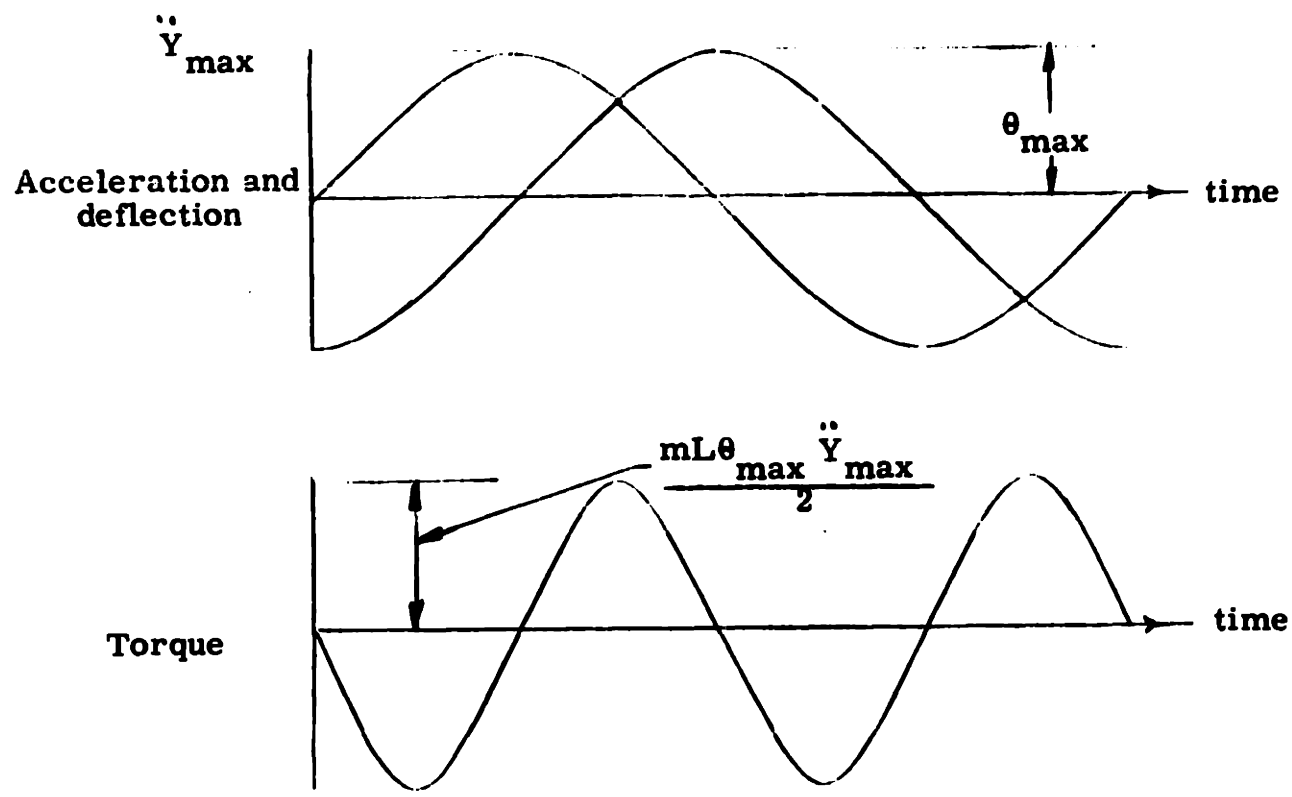
Acceleration, deflection, and pendulum torque vs. time for deflection lagging acceleration by 90°

Fig. 3-8

Figure 3-8 shows that the pendulum torque varies at twice the excitation frequency and that the average torque over a cycle of vibration is equal to $\frac{mL\theta_{max} \ddot{Y}_{max}}{2}$.

This average torque indicates that the pendulum is oscillating about an axis other than the pendulum reference

When the pendulum deflection lags the acceleration input by 90° as illustrated in Fig. 3-9, there is no average pendulum torque over a cycle of vibration and the pendulum will oscillate about its reference axis.



$$\text{pendulum torque} = mL\theta\ddot{Y} = - \frac{mL\theta_{max} \ddot{Y}_{max}}{2} \sin 2 \omega t$$

Fig. 3-9

Acceleration, vibration, and torque vs. time for a simple pendulum whose displacement lags applied acceleration by 90°

The variation of vibropendulum torque with vibration frequency as given by equation (3-9) and plotted in Fig. 3-6 can be explained quantitatively with the aid of Figs. 3-7 to 3-9.

For a pendulum having elastic restraint and damping

a. The pendulum motion will be in phase with the applied acceleration at low vibration frequencies as illustrated in Figs. 3-7 and 3-8. For a given magnitude of acceleration, the maximum vibropendulum error will occur at zero frequency; and an error equal to one half the cross-coupling error of Section 3. 2 will occur.

b. At vibration frequencies equal to $\sqrt{\frac{K}{I}}$, the pendulum deflection will lag the applied acceleration by 90° . There will be no average torque over a cycle of vibration and no vibropendulum error as illustrated in Fig. 3-9.

c. At vibration frequencies greater than $\sqrt{\frac{K}{I}}$, the pendulum deflection will lag the acceleration by more than 90° . A negative vibropendulum torque occurs. The vibropendulum torque will asymptotically approach zero with increasing vibration frequencies.

CHAPTER 4

CROSS-COUPLING AND VIBROPENDULUM LIX ERRORS OBTAINED FOR SMALL ROTATION OF THE CONTROL-MEMBER AXIS

4.1 INTRODUCTION

The errors of the linear integrating accelerometer under constant and vibratory accelerations are determined. Errors are determined for small rotation of the control-member axis. It is assumed that the frequency of vibration is such that many cycles of vibration occur during this small angle of control-member rotation.

The errors are determined for the following two control-member drive performance functions, a constant, and an integrator.

4.2 EQUATION OF MOTION OF LIX SUBJECTED TO A TRANSLATIONAL ACCELERATION

For this initial derivation, it is assumed that the gyro unit input axis is perfectly aligned with the control-member axis. It is also assumed that the accelerometer base is mounted on a stabilized platform and therefore isolated from angular velocities and angular accelerations with respect to inertial space.

The sum of the torques acting on the LIX gyro float (torque summing member) for small float deflection angles is given by

$$I\ddot{\theta} + C_d\dot{\theta} + H\omega_{cm} = mL\ddot{X} + mL\dot{Y}\theta \cos A_{cm} \quad (4-1)$$

where

I = moment of inertia of gyro float about its output axis (gm-cm^2)

θ = float displacement angle about the gyro output axis measured from the position where the pendulum axis is perpendicular to the control-member axis (radians)

C_d = rotational damping coefficient of the gyro float about its output axis (dyne-cm/rad/sec)

mL = float pendulosity along the gyro spin axis (gm-cm)

\ddot{X} = component of acceleration parallel to control-member axis of LIX unit (cm/sec^2)

\ddot{Y} = component of acceleration perpendicular to the control-member axis of LIX unit (cm/sec^2)

H = angular momentum of pendulous gyro wheel ($\text{gm-cm}^2/\text{sec}$)

ω_{cm} = angular velocity of control member (radians/sec)

A_{cm} = control-member angle measured from the position

where the pendulous arm (ideal) is coincident

with \ddot{Y} (radians)

A block diagram of the LIX system is shown in Fig. 4-1.

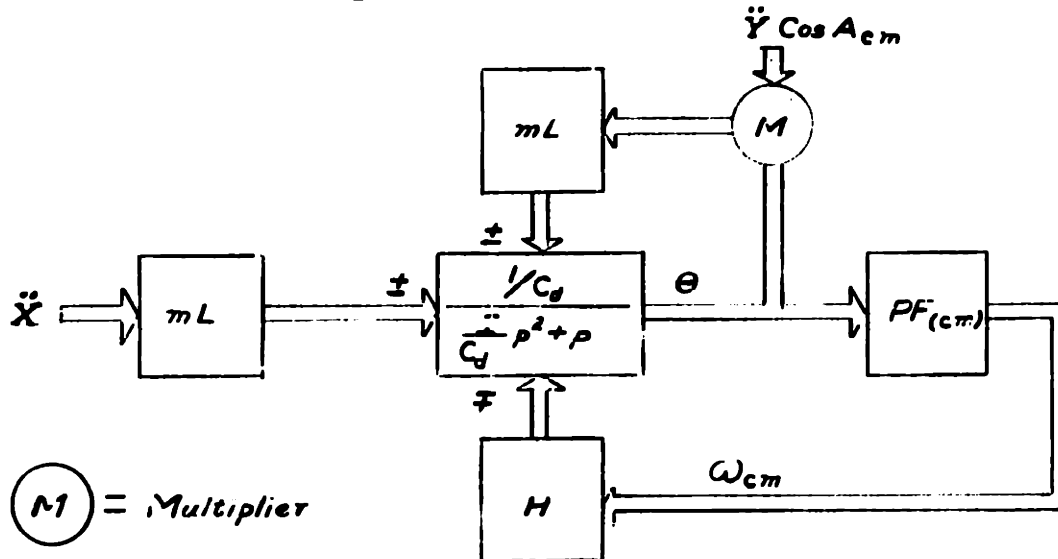


Fig. 4-1

Block diagram of LIX system

If the ratio of control-member angular velocity and vibration frequencies are such that the control member turns through a small angle during several cycles of vibration, the $\cos A_{cm}$ term of equation (4-1) will be essentially constant over the interval for which equation (4-1) is solved. For this case, $\cos A_{cm}$ term can be included with other constant portions of the \ddot{Y} term, equation (4-1) will be of the form

$$I\ddot{\theta} + C_d\dot{\theta} + H\omega_{cm} = mL\ddot{X} + mL\ddot{Y}'\theta \quad (4-2)$$

where

$$\ddot{Y}' = \ddot{Y} \cos A_{cm}$$

As shown in Fig. 4-1, the control-member angular velocity is related to the gyro float angular displacement by the relationship

$$\omega_{cm} = PF_{(cm)} \dot{\theta} \quad (4-3)$$

where

$PF_{(cm)}$ = the performance function of the control-member drive. $PF_{(cm)}$ is derived for the LIX unit in Chapter 7.

The LIX unit subjected to a combination of translational acceleration and vibration will now be analyzed for two control-member drive performance functions: a constant and an integrator.

4.3 CONTROL-MEMBER PERFORMANCE FUNCTION, A CONSTANT

The performance function of the control member is represented by a constant gain, G . For this case, equation (4-2) becomes

$$I\ddot{\theta} + C_d\dot{\theta} + HG\theta = mL\ddot{X} + mL\ddot{Y}'\theta \quad (4-4)$$

Equation (4-4) is the equation of motion of a pendulum with a restraint (HG) and a damping (C_d) subjected to an acceleration input \ddot{X} parallel to the pendulum sensitive axis and an acceleration \ddot{Y}' perpendicular to the pendulum sensitive direction for the condition of a small pendulum deflection angle (θ).

If the acceleration input is of the form

$$\begin{aligned}\ddot{X} &= B \sin \omega t + E \\ \ddot{Y} &= A \sin \omega t + D\end{aligned}\quad (4-5)$$

Equation (4-4) becomes

$$I\ddot{\theta} + C_d\dot{\theta} + (HG - mL A \sin \omega t - D mL) \theta = mL[B \sin \omega t + E] \quad (4-6)$$

Equation (4-6) is a linear equation with time varying coefficients. As discussed in references 6, 7, and 8, there is no closed-form solution of equation (4-6). If the constants $\frac{I}{C_d}$, $\frac{mLA}{C_d}$, $\frac{mLD}{C_d}$, $\frac{mLB}{C_d}$, and $\frac{mLE}{C_d}$ are much smaller than unity, the method of solution illustrated in reference 6 can be used to solve equation (4-6). This iteration method has been carried out for this equation in Appendix A Section A. 2. The following results were obtained.

The value of float deflection angle ($\bar{\theta}$) averaged over a cycle of vibration is

$$\bar{\theta} = \frac{mLE}{HG - mL D} + \frac{(mL)^2 (HG - mL D - I\omega^2) AB}{2(HG - mL D) \left[C_d^2 \omega^2 + (HG - mL D - I\omega^2)^2 \right]}$$

(4-7)

At low vibration frequencies

where

$$\omega \ll \sqrt{\frac{HG - mL D}{I}}$$

$$\omega \ll \frac{HG - mL D}{C_d}$$

and if $\frac{mLD}{HG} \ll 1$, equation (4-7) becomes

$$\text{Pendulum torque} = HG\bar{\theta} = mL\bar{E} + \frac{(mL)^2 AB}{2GH} + \frac{(mL)^2 DE}{HG} \quad (4-8)$$

The three terms in the solution are

1) $mL\bar{E}$ = torque required to react the average value of acceleration along the "X" direction. This is the only acceleration that should produce a torque, any other terms are errors.

2) $\frac{(mL)^2 DE}{HG}$ = cross-coupling torque caused by the Y component of acceleration exerting a torque on the pendulum when it is not in its null position.

3) $\frac{(mL)^2 AB}{2HG}$ = vibropendulum torque. This term results from a torque rectification due to vibration input. (Note the similarity in form to the cross-coupling term.)

When the control-member performance function is a constant, there is a cross-coupling and vibropendulum error torque. These error torques decrease with increasing loop gain (HG). A sufficiently high loop gain must be used so that the cross-coupling and vibropendulum errors are below the accuracy requirement for the instrument.

The vibropendulum torque can be separated from the cross-coupling torque in equation (4-7) if $mLD \ll HG$. For this case, the variation in vibropendulum torque with frequency is given by

$$M_{(vp)} = \frac{(mL)^2 (GH - I\omega^2) AB}{2 \left[(C_d^2 \omega^2) + (GH - I\omega^2)^2 \right]} \quad (4-9)$$

If $C_d^2 \gg GH$, the maximum vibropendulum torque occurs at low vibration frequencies

where

$$\omega \ll \sqrt{\frac{HG}{I}}$$

and

$$\omega \ll \frac{HG}{C_d}$$

$$M_{(vp)(max)} = \frac{(mL)^2 AB}{2GH} \quad (4-10)$$

Figure 3-6 is a plot of the variation of vibropendulum with frequency. A family of curves have been plotted for various values of $\frac{C_d^2}{GHI}$ where the restraint GH has been represented by K.

4.4 CONTROL-MEMBER PERFORMANCE FUNCTION, AN INTEGRATOR

With the control-member performance function an integrator, the angular velocity of the control member can be related to the float deflection by the relationship

$$\omega_{cm} = G \int \theta dt \quad (4-11)$$

Substituting equation (4-11) into equation (4-2) obtains

$$I\ddot{\theta} + C_d \dot{\theta} + HG \int \theta dt = mL \ddot{X} + mL \theta \ddot{Y}' \quad (4-12)$$

Differentiating equation (4-12)

$$I\ddot{\theta} + C_d\dot{\theta} + HG\theta = mL\ddot{X} + mL\dot{\theta}\ddot{Y}' + mL\dot{\theta}'\ddot{Y}' \quad (4-13)$$

The input consisting of a constant acceleration and a vibratory acceleration at some angle to the pendulum axis is given by equation (4-5). With this input, equation (4-13) becomes

$$\tau\ddot{\theta} + \dot{\theta} - \dot{\theta}[a \sin \omega t + d] + (k - a\omega \cos \omega t)\theta = b\omega \cos \omega t \quad (4-14)$$

where

$$\tau = \frac{I}{C_d} \quad a = \frac{mLA}{C_d} \quad d = \frac{mLD}{C_d} \quad k = \frac{HG}{C_d} \quad (4-15)$$

The solution of equation (4-14) can be obtained as the series

$$\theta = \theta_1 + \theta_3 + \theta_5 + \dots + \theta_{(2m-1)} + \theta_{2m} \quad (4-16)$$

where

$$\tau\ddot{\theta}_1 + \dot{\theta}_1 + k\theta_1 = b\omega \cos \omega t \quad (4-17)$$

$$\tau\ddot{\theta}_3 + \dot{\theta}_3 + k\theta_3 = (a \sin \omega t + d)\dot{\theta}_1 + (a\omega \cos \omega t)\theta_1 \quad (4-18)$$

$$\tau\ddot{\theta}_5 + \dot{\theta}_5 + k\theta_5 = (a \sin \omega t + d)\dot{\theta}_3 + (a\omega \cos \omega t)\theta_3 \quad (4-19)$$

Consecutively to

$$\begin{aligned} \tau \ddot{\theta}_{(2m-1)} + \ddot{\theta}_{(2m-1)} + k\theta_{(2m-1)} &= (a \sin \omega t + d) \dot{\theta}_{(2m-3)} \\ &+ (a \omega \cos \omega t) \theta_{(2m-3)} \end{aligned} \quad (4-20)$$

$$\begin{aligned} \tau \ddot{\theta}_{2m} + \ddot{\theta}_{2m} - \dot{\theta}_{2m} (a \sin \omega t + d) &+ (k - a \omega \cos \omega t) \theta_{2m} \\ &= (a \sin \omega t + d) \dot{\theta}_{(2m-1)} + (a \omega \cos \omega t) \theta_{(2m-1)} \end{aligned} \quad (4-21)$$

The solution of equation (4-17) is of the form

$$\theta_1 = E \sin \omega t + F \cos \omega t \quad (4-22)$$

Substituting equation (4-22) into equation (4-18) yields

$$\begin{aligned} \tau \ddot{\theta}_3 + \ddot{\theta}_3 + k\theta_3 &= -dF\omega \sin \omega t + dE \omega \cos \omega t \\ &aE \omega \sin 2\omega t + a\omega F \cos 2\omega t \end{aligned} \quad (4-23)$$

The solution of equation (4-23) is of the form

$$\theta_3 = L \sin \omega t + M \cos \omega t + N \sin 2\omega t + O \cos 2\omega t \quad (4-24)$$

In a similar manner, the solutions of equation (4-19) to (4-20) can be obtained.

Successive terms in the solution of θ will be harmonics of the vibration frequency.

The convergence and stability of the solution can be shown by the method of Appendix A.

Since the float deflection angle will be periodic, there is no average deflection, cross-coupling, or vibropendulum error over a cycle of vibration .

Similarly it can be shown that there will be no average float deflection angle or vibropendulum error if the control-member performance function is an integrator of any order greater than one.

In the control-member frequency range for which the performance function of the control-member drive is a constant, there will be a crosscoupling and vibropendulum error. In the frequency range for which the performance function is an integrator, there is no cross-coupling or vibropendulum error. Therefore, a conservative error analysis is obtained by assuming the control-member performance function is a constant.

Consider a linear integrating accelerometer whose unit axes are perfectly aligned. If an integrator is added to the control-member drive system so that the performance function is an integrator at zero frequency and an integrator of the order greater than one at other frequencies, there will be no cross-coupling and vibropendulum errors.

Therefore, this is the desired performance function. This situation for the LIX loop is discussed in Chapter 7.

CHAPTER 5

CROSS-COUPLING, VIBROPENDULUM, AND MISALIGNMENT LIX ERRORS AVERAGED OVER A PERIOD OF CONTROL- MEMBER ROTATION

5.1 INTRODUCTION

It is shown in Chapters 3 and 4 that an acceleration applied at an angle to the sensitive axis of a restrained pendulum causes an error in the measurement of the true acceleration. This error is the cross-coupling error.

Similarly a vibration applied at an angle to the restrained pendulum's sensitive axis causes an error torque that is referred to as the vibropendulum error.

A misalignment angle between the LIX gyro input and control-member axes allows a component of acceleration perpendicular to the control-member axis to act along the pendulum sensitive axis. This error torque has been named the misalignment torque and occurs even if the pendulum has an infinite elastic restraint.

The results obtained for the analysis of the restrained pendulum can be applied directly to the LIX unit if the LIX control member is not rotating. This is shown in Chapter 4.

If the control member of the LIX unit is rotating, the pendulous torque caused by the component of acceleration perpendicular to the sensitive axis of the pendulum will be modified by the control-member angle. The perpendicular component of acceleration will cause an error in control-member rate and in the indicated acceleration.

The errors in the measurement of true acceleration for the LIX unit with a finite pendulum elastic restraint due to the cross-coupling torque, vibropendulum torque, or misalignment torque averaged over complete revolutions of the control member is determined in this chapter.

5.2 CROSS-COUPLING ERROR FOR CONDITION OF PERFECT UNIT ALIGNMENT

If the performance function of the control-member drive is a constant (G), the LIX unit will experience a cross-coupling error for an acceleration applied at an angle to the pendulum sensitive axis as shown in Chapter 4. The cross-coupling error averaged over complete revolutions of the control member is determined in this section.

In this case, the float elastic restraint will be HG (as shown for equation (4-4)), where H is the gyro wheel angular momentum.

The float deflection angle, θ_s , due to an acceleration a_{in} applied along the pendulum sensitive axis is

$$\theta_s = \frac{mL}{HG} a_{in} \quad (5-1)$$

This float deflection angle, θ_s , will allow the component of acceleration that is perpendicular to the control-member axis

to cause a cross-coupling torque. This cross-torque components will be modified by the cosine of the control-member angle. This is illustrated in Fig. 5-1.

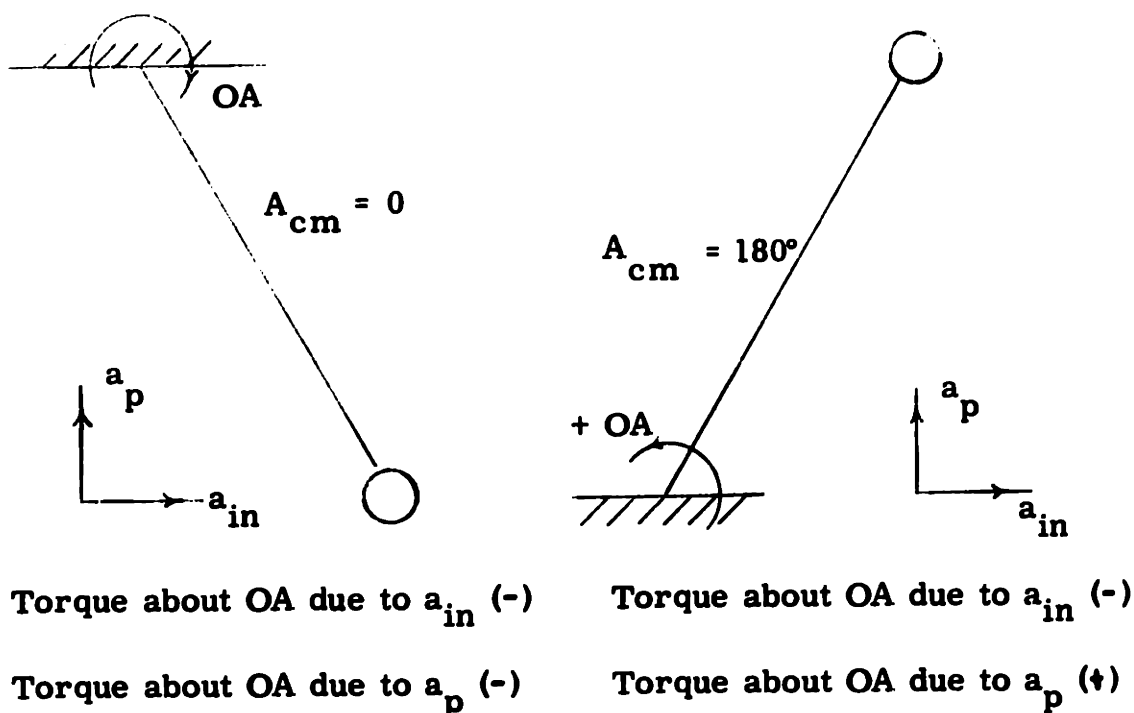


Fig. 5-1

Modification of LIX torques with control-member rotation

When the LIX unit is subjected to an acceleration (a_{in}) parallel to the control-member axis and an acceleration (a_p) perpendicular to the control-member axis, the sum of the torques acting on the gyro float (from equation (4-1)) becomes

$$I\ddot{\theta} + C_d\dot{\theta} + H\omega_{cm} = mL \left[a_{in} + a_p \theta \cos A_{cm} \right] \quad (5-2)$$

The elastic restraint about the output axis is designed to be large.* Therefore, the static deflection angle (θ_s) due to the component of acceleration along the pendulum sensitive axis will be small. If a_p and a_{in} are of the same order of magnitude, the component of acceleration parallel to the control-member axis, a_{in} , will be much greater than the cross-coupling term, $a_p \theta \cos A_{cm}$. Therefore, the pendulum is very nearly displaced a small angle from null, θ_s , due to the constant forcing input, $mL a_{in}$; and the oscillating term, $mL a_p \theta \cos A_{cm}$, will cause a negligible change in this angular deflection. For this reason $\ddot{\theta}$ and $\dot{\theta}$ will very nearly be equal to zero; and equation (5-2) becomes

$$H\omega_{cm} = mL (a_{in} + a_p \theta_s \cos A_{cm}) \quad (5-3)$$

or

$$\omega_{cm} = \frac{dA_{cm}}{dt} = \frac{mL}{H} (a_{in} + a_p \theta_s \cos A_{cm}) \quad (5-4)$$

Separating variables of equation (5-4) yields

$$dt = \frac{dA_{cm}}{\frac{mL}{H} (a_{in} + a_p \theta_s \cos A_{cm})} \quad (5-5)$$

The control-member period (the time for the control member to make one revolution) is obtained by integrating equation (5-5) over 2π radians

$$T = \int_0^{2\pi} \frac{dA_{cm}}{\frac{mL}{H} (a_{in} + a_p \theta_s \cos A_{cm})} \quad (5-6)$$

*See Chapter 5 of volume II for the value of the LIX restraint.

Integrating equation (5-6) between 0 and 2π yields

$$T = \frac{2\pi}{\frac{mL}{H} a_{in} \sqrt{1 - \left(\frac{a_p}{a_{in}} \theta_s\right)^2}} \quad (5-7)$$

Since the average angular velocity is defined as $\frac{2\pi}{\text{period}}$,

the control-member average angular rate, $\omega_{(cm)(av)}$, is

$$\omega_{(cm)(av)} = \frac{mL}{H} a_{in} \sqrt{1 - \left(\frac{a_p}{a_{in}} \theta_s\right)^2} \quad (5-8)$$

$\frac{mL}{H} a_{in}$ is the desired control-member rate for no cross-coupling error as shown in Chapter 2.

Therefore, the indicated acceleration, $A_{(ind)(av)}$, averaged over a revolution of the control member is

$$A_{(ind)(av)} = a_{in} \sqrt{1 - \left(\frac{a_p}{a_{in}} \theta_s\right)^2} \quad (5-9)$$

For small values of $\left(\frac{a_p}{a_{in}} \theta_s\right)$, equation (5-9) is approximated by

$$A_{(ind)(av)} \approx a_{in} \left[1 - 1/2 \left(\frac{a_p}{a_{in}} \theta_s\right)^2 \right] \quad (5-10)$$

From equation (5-10), the dimensionless error in measured acceleration averaged over a revolution of the control member, $A_{(meas)(error)(av)}$ is nearly equal to

$$A_{(meas)(error)(av)} \approx \frac{1}{2} \left(\frac{a_p}{a_{in}} \theta_s\right)^2 \quad (5-11)$$

Combining equations (5-1) and (5-11), the average error in measured acceleration equals

$$A_{(\text{meas})(\text{error})(\text{av})} \approx \frac{1}{2} \left(a_p \frac{mL}{HG} \right)^2 \quad (5-12)$$

From equation (4-8), the cross-coupling and desired pendulum torques were found to be

$$M_{(\text{cp})} = \frac{(mL)^2 a_{\text{in}} a_p}{HG} \quad (5-13)$$

$$M_{(\text{desired})} = mL a_{\text{in}} \quad (5-14)$$

Substituting equations (5-13) and (5-14) into equation (5-12) yields

$$A_{(\text{meas})(\text{error})(\text{av})} = \frac{1}{2} \left(\frac{M_{(\text{cp})}}{M_{(\text{desired})}} \right)^2 \quad (5-15)$$

If there is no control-member rotation, the error in measured acceleration would be

$$A_{(\text{meas})(\text{error})} = \frac{M_{(\text{cp})}}{M_{(\text{desired})}} \quad (5-16)$$

Since the cross-coupling torque, $M_{(\text{cp})}$, is generally much less than the desired torque, $M_{(\text{desired})}$, $\frac{M_{(\text{cp})}}{M_{(\text{desired})}}$ will generally be much less than unity; and the acceleration error averaged over a revolution of the control member will be less than the acceleration error for a pendulum unit without a rotating control member. Therefore, a LIX unit will have a smaller cross-coupling error than a pendulum accelerometer having the same elastic restraint.

Actual cross-coupling errors for the LIX unit have been calculated in Chapter 5 of Volume II.

5.3 CROSS-COUPLING ERROR DUE TO MISALIGNMENT BETWEEN LIX GYRO INPUT AND CONTROL-MEMBER AXES

The magnitude of accelerometer error resulting from misalignments between the LIX gyro input and control-member axes is derived in this section.

If the input axis of the gyro is not perfectly aligned with the control-member axis; the unit is subjected to an acceleration, a_{in} , parallel to the control-member axis; and an acceleration, a_p , normal to the control-member axis, equation (5-2) becomes

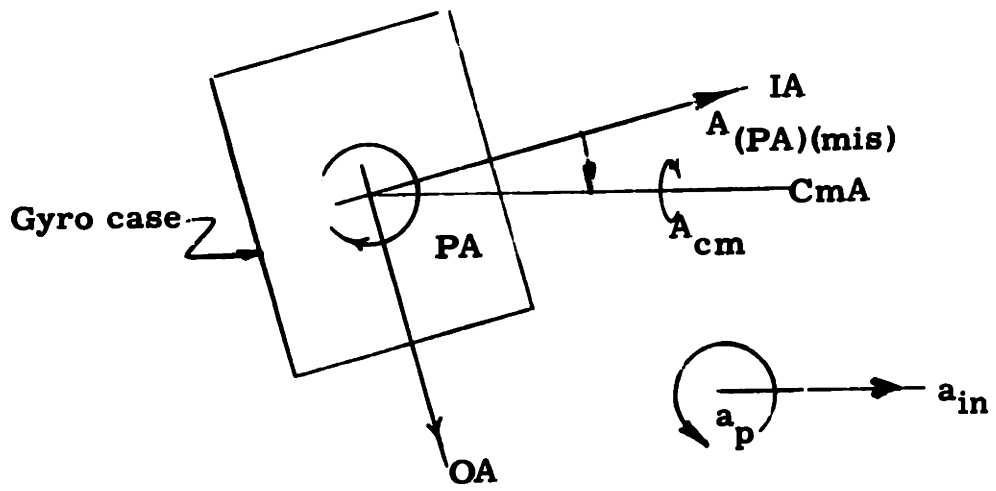
$$I\ddot{\theta} + C_d\dot{\theta} + H\omega_{cm} = mL \left[a_{in} \cos (A_{(OA)(mis)} + A_{(PA)(mis)}) + a_p \sin A_{(OA)(mis)} \cos A_{cm} + a_p \sin A_{(PA)(mis)} \sin A_{cm} \right] \quad (5-17)$$

where

$A_{(OA)(mis)}$ = misalignment angle between LIX gyro input and control-member axes measured about the gyro output axis. This angle is composed of two components. One component is the float deflection angle, the other is a misalignment between the gyro unit case and the control member of the LIX.

$A_{(PA)(mis)}$ = misalignment angle between the LIX gyro input and control-member axis measured about the gyro pendulum axis.

The misalignment angles are illustrated in Fig. 5-2.



$A_{cm} = 0$

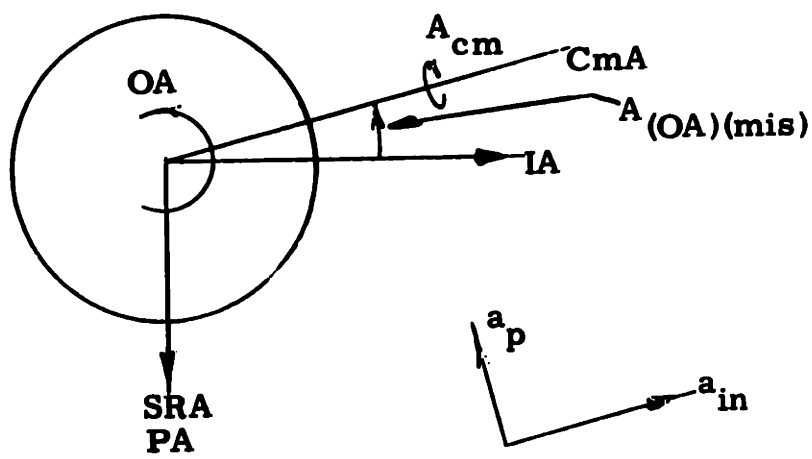


Fig. 5-2

Misalignment angles of LIX unit

For small misalignment angles, equation (5-17)

becomes

$$I\ddot{\theta} + C\dot{\theta} + H\omega_{cm} = mL \left[a_{in} + a_p A_{(OA)(mis)} \cos A_{cm} + a_p A_{(PA)(mis)} \sin A_{cm} \right] \quad (5-18)$$

$$= mL \left[a_{in} + a_p A_{(mis)} \cos (A_{cm} - \tau) \right] \quad (5-19)$$

where

$$A_{(mis)} = \left(A_{(OA)(mis)}^2 + A_{(PA)(mis)}^2 \right)^{1/2}$$

$$\tau = \tan^{-1} \frac{A_{(PA)(mis)}}{A_{(OA)(mis)}}$$

Using the method of Section 5, 1, the average dimensionless error in measured acceleration due to this misalignment for the acceleration input averaged over a revolution of the control member would be approximately given by

$$A_{(meas)(error)(av)} = \frac{1}{2} \left(\frac{a_p}{a_{in}} \right)^2 \left(A_{(OA)(mis)}^2 + A_{(PA)(mis)}^2 \right) \quad (5-20)$$

If there is no control-member rotation, the error in measured acceleration due to this misalignment is

$$A_{(meas)(error)} = \frac{a_p}{a_{in}} \left(A_{(OA)(mis)}^2 + A_{(PA)(mis)}^2 \right)^{1/2} \quad (5-21)$$

Since the misalignment angles are generally very small, the error in measured acceleration averaged over a rotation of the control member is generally less than the

misalignment errors for a pendulum accelerometer without a rotating control member.

The degree of precision necessary for alignment of the unit axes is dictated by the accuracy requirement of the accelerometer.

5.4 VIBROPENDULUM ERROR FOR LIX UNIT SUBJECTED TO VIBRATION AT AN ANGLE TO THE CONTROL-MEMBER AXIS

In some guidance systems (see reference 11), the input axis of one accelerometer is maintained perpendicular to the direction of flight. The autopilot corrects the vehicle for any acceleration indicated by this accelerometer. Ideally, the output of this accelerometer is maintained equal to zero; and this unit's control member will not be turning during flight. In this section, it will be shown that a vibration input to this accelerometer will be indicated as a velocity error and will cause an error in vehicle heading at cutoff.

Consider the LIX unit subjected to a vibration input, \ddot{X} parallel to the LIX control-member axis, and \ddot{Y} perpendicular to the LIX control-member axis of the form

$$\begin{aligned}\ddot{X} &= D \sin \omega t \\ \ddot{Y} &= A \sin \omega t + B \cos \omega t\end{aligned}\tag{5-22}$$

The sum of the torques acting on the LIX gyro float when subjected to the input of equation (5-22) would be given by

$$I\ddot{\theta} + C_d\dot{\theta} + H\omega_{cm} = mL \left[D \sin \omega t + \theta (A \sin \omega t + B \cos \omega t) (\cos A_{cm}) \right]\tag{5-23}$$

As shown in Chapter 7, at low-control-member frequencies, the control-member angular velocity (ω_{cm}) is related to the deflection angle (θ) of the pendulous gyros float by the steady-state gain (G) of the servo components connecting the float signal generator to the control-member drive motor or

$$\omega_{cm} = G\theta \quad (5-24)$$

Substituting equation (5-24) into equation (5-23) obtains

$$I\ddot{\theta} + C_d\dot{\theta} + GH\theta = mL[D \sin \omega t + (A \sin \omega t + B \cos \omega t)\theta \cos A_{cm}] \quad (5-25)$$

Since the instrument being analyzed in this section is oriented to maintain zero-control-member rotation, $\cos A_{cm}$ does not change much during several cycles of vibration and can be included in the constants A and B.

Equation (5-25) is the equation of motion of a pendulum having a restraint (GH) and a damping (C_d) subjected to the vibration input of equation (5-22). The pendulum subjected to this input is analyzed in detail in Appendix A.

It is found that at low frequencies where $\omega^2 \ll \frac{GH}{I}$, $\omega \ll \frac{GH}{C_d}$, and $\omega \ll \frac{GHA}{C_d B}$, the pendulum experiences the largest float deflection angle. This angle averaged over a vibration cycle is given by

$$\theta = \frac{(mL)^2 AD}{(GH)^2} \quad (5-26)$$

For the LIX unit, equation (5-25) shows that the component of vibration perpendicular to the control-member axis is reduced by $\cos A_{cm}$. Therefore, the float deflection angle (θ) becomes

$$\theta = \frac{(mL)^2 AD}{(GH)^2} \cos A_{cm} \quad (5-27)$$

Combining equations (5-24) and (5-27) yields

$$\omega_{cm} = \frac{(mL)^2 AD \cos A_{cm}}{GH^2} \quad (5-28)$$

Since $\omega_{cm} = \frac{dA_{cm}}{dt}$, equation (5-28) can be put into the form

$$dt = \frac{dA_{cm}}{\frac{(mL)^2 AD}{GH^2} \cos A_{cm}} \quad (5-29)$$

The time, $t_{A'_{cm}}$, for the control member to rotate through an angle, A'_{cm} , is given by

$$t_{A'_{cm}} = \frac{GH^2}{(mL)^2 AD} \int_0^{A'_{cm}} \frac{dA_{cm}}{\cos A_{cm}} \quad (5-30)$$

or

$$t_{A'_{cm}} = \frac{GH^2}{(mL)^2 AD} \log \tan \left(\frac{\pi}{4} + \frac{A'_{cm}}{2} \right) \quad (5-31)$$

Equation (5-31) can only be evaluated for A'_{cm} less than 90° since the tangent function is discontinuous at 90° .

Equation (5-31) shows that it takes an infinite time for the control member to turn through an angle of 90° . If the

vibration input given by equation (5-22) maintains a constant orientation with the control-member axis, the control member will never turn through an angle of 90°.

The relationship between vehicle velocity, v_{in} , and control-member angular displacement is obtained from Chapter 2.

$$A'_{cm} = \frac{mL}{H} \int_0^t a_{in} dt \quad (2-3) \text{ repeated}$$

If $A'_{cm} = 0$ when $v_{in} = 0$

$$A'_{cm} = \frac{mL}{H} v_{in} \quad (5-32)$$

Since for the case considered, the control member never turns through an angle of 90°, the maximum indicated velocity, v_{max} , becomes

$$v_{max} = \frac{\pi H}{2mL} \quad (5-33)$$

Substituting equation (5-32) into equation (5-31) yields

$$t_{A'_{cm}} = \frac{GH^2}{(mL)^2 AD} \log \tan \left(\frac{\pi}{4} + \frac{mL v_{in}}{2H} \right) \quad (5-34)$$

The variation in indicated vehicle acceleration with time can be obtained for any gyro pendulum accelerometer from equation (5-34).

A plot of this equation is shown in Fig. 5-3.

From equation (5-31), the time for the control member to turn through an angle of 89°, for which a velocity error of (89/90) v_{max} would be obtained is

$$t_{89^\circ} = \frac{4.74 GH^2}{(mL)^2 AD} \quad (5-35)$$

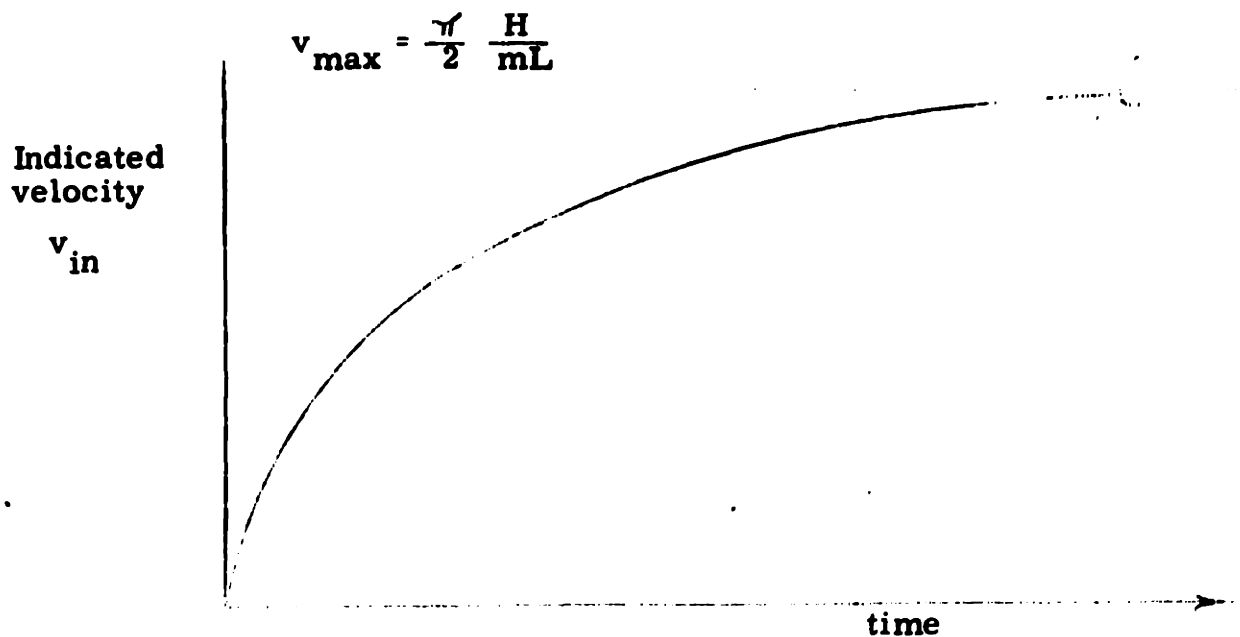


Fig. 5-3

Velocity error vs. time for LIX unit subjected to vibration input

5. 5 VIBROPENDULUM ERROR FOR VIBRATION APPLIED AT AN ANGLE TO CONTROL-MEMBER AXIS WHILE A CONSTANT ACCELERATION IS BEING APPLIED ALONG LIX INPUT AXIS

If an accelerometer is mounted with its input axes in the intended plane of vehicle flight, it will have a continuously turning control member during powered flight. The vibropendulum errors for an instrument with a continuously rotating control member is analyzed in this section.

Consider the LIX unit subject to an acceleration parallel to the control-member axis (\ddot{X}) and an acceleration perpendicular to the control-member axis (\ddot{Y}) as given by

$$\ddot{X} = B \sin \omega t + E$$

$$\ddot{Y} = A \sin \omega t \tag{5-36}$$

The sum of the torques acting on the LIX gyro float is given by

$$I\ddot{\theta} + C_d\dot{\theta} + H\omega_{cm} = mL \left[B \sin \omega t + E + \theta (A \sin \omega t) \cos A_{cm} \right] \quad (5-37)$$

At low control-member frequencies (from the discussion for equation (5-24))

$$\omega_{cm} = G\theta \quad (5-24) \text{ repeated}$$

Substituting equation (5-24) into equation (5-37) obtains

$$I\ddot{\theta} + C_d\dot{\theta} + GH\theta = mL \left[B \sin \omega t + E + \theta (A \sin \omega t) \cos A_{cm} \right] \quad (5-38)$$

If the ratio of control-member angular velocity and vibration frequencies are such that the control member turns through a small angle during several cycles of vibration, the $\cos A_{cm}$ term can be considered constant for the interval for which equation (5-38) is solved. The $\cos A_{cm}$ term can be included in the value of the constant A. For this case, equation (5-38) is the equation of motion of a pendulum having a restraint (HG) and a damping (C_d) subjected to the acceleration input of equation (5-36). The pendulum subjected to this acceleration input has been analyzed in detail in Appendix A. It can be shown that the pendulum will experience a constant angular deflection of the form

$$\theta = \frac{mLE}{GH} + \frac{(mL)^2 (1 - \mu) AB}{2 \left[\frac{C_d^2}{GH} \mu + (1 - \mu)^2 \right] G^2 H^2} \quad (5-39)$$

where

$$\mu = \frac{\omega_1^2}{GH}$$

Combining equations (5-24) and (5-39) and modifying the "Y" component of acceleration by $\cos A_{cm}$ obtains

$$\omega_{cm} = \frac{\theta}{G} = \frac{mLE}{H} + \frac{(mL)^2 (1-\mu) AB \cos A_{cm}}{2 \left[\frac{C_d^2}{GHI} \mu + (1-\mu)^2 \right] GH^2} \quad (5-40)$$

Using the method of Section 5.2, equation (5-40) can be solved to yield the error in measured acceleration averaged over a revolution of the control member

$$A_{(meas)(error)(av)} = \frac{1}{2} \left(\frac{(mL)(1-\mu)AB}{2 \left[\frac{C_d^2}{GHI} \mu + (1-\mu)^2 \right] EGH} \right)^2 \quad (5-41)$$

Comparing equation (5-41) to equation (3-9) for the vibropendulum torque ($M_{(vp)}$), equation (5-41) can be written as

$$A_{(meas)(error)(av)} = \frac{1}{2} \left(\frac{M_{(vp)}}{M_{(desired)}} \right)^2 \quad (5-42)$$

With no control member rotation, the accelerometer error due to the vibropendulum torque equals

$$A_{(meas)(error)} = \frac{M_{(vp)}}{M_{(desired)}} \quad (5-43)$$

Since $M_{(vp)}$ is generally much less than $M_{(desired)}$, comparing equations (5-42) and (5-43), the vibropendulum error averaged over a rotation of the control member is generally less than the vibropendulum error for a pendulum unit without a rotating control member.

Figure 3-6 is a dimensionless plot of the variation of vibropendulum torque with vibration frequency. From this graph, the acceleration error for any gyro pendulum or pendulum accelerometer can be obtained. At low control-member frequencies where

$$\omega^2 \ll \frac{GH}{I}$$

and

$$\omega \ll \frac{GH}{C_d}$$

The error in measured acceleration averaged over a rotation of the control member is

$$A_{(meas)(error)(av)} = \frac{1}{8} \left(\frac{mLAB}{GHE} \right)^2 \quad (5-44)$$

Without the control member rotating at this low frequency range, the acceleration error is

$$A_{(meas)(error)} = \frac{mLAB}{2GHE} \quad (5-45)$$

5.6 VIBROPENDULUM ERROR FOR MISALIGNMENT BETWEEN LIX GYRO INPUT AND CONTROL-MEMBER AXES

It is shown in this section that a small misalignment angle, $A_{(OA)(mis)}$, between the LIX gyro input and control-

member axis will cause a negligible increase in vibropendulum error.

When the LIX unit, having a misalignment angle, $A'_{(OA)(mis)}$ (a fixed misalignment about OA between the gyro unit case and the control-member of the LIX), is subjected to a vibration input of the form

$$\begin{aligned}\ddot{X} &= D \sin \omega t \\ \ddot{Y} &= A \sin \omega t\end{aligned}\quad (5-46)$$

The sum of the torques acting on the gyro float is given by

$$\begin{aligned}I\ddot{\theta} + C_d\dot{\theta} + H\omega_{cm} &= mL \left[D \sin \omega t \cos \left(\theta + A'_{(OA)(mis)} \right) \right. \\ &\left. + \sin \left(\theta + A'_{(OA)(mis)} \right) A \sin \omega t \cos A_{cm} \right]\end{aligned}\quad (5-47)$$

The control-member angular velocity (ω_{cm}) is related to the gyro float angular deflection (θ) by the performance function of the control-member drive. At low control-member frequencies

$$\omega_{cm} = G\theta \quad (5-24) \text{ repeated}$$

If the ratio of control-member angular velocity and vibration frequencies are such that the control member turns through a small angle during a cycle of vibration, the $\cos A_{cm}$ term of equation (5-47) will be essentially constant over the interval for which the equation is solved. With the above assumption

and the following two assumptions (1) the performance function of the control-member drive is a constant G , (2) the float deflection angle, θ , and misalignment angle, $A'_{(OA)(mis)}$, are small, equation (5-47) becomes

$$I\ddot{\theta} + C_d\dot{\theta} + HG\theta = mL \left(D \sin \omega t - \theta A'_{(OA)(mis)} D \sin \omega t + \theta A \sin \omega t + A'_{(OA)(mis)} A \sin \omega t \right) \quad (5-48)$$

Where it is assumed, the $\cos A_{cm}$ term is included in the appropriate constants. Dividing through by C_d and rearranging terms yields

$$\tau\ddot{\theta} + \dot{\theta} + \theta(k' - a' \sin \omega t) = d' \sin \omega t \quad (5-49)$$

where

$$k' = \frac{HG}{C_d} \quad (5-50)$$

$$\tau = \frac{I}{C_d} \quad (5-51)$$

$$a' = \frac{mL}{C_d} \left[A - D A'_{(OA)(mis)} \right] \quad (5-52)$$

$$d' = \frac{mL}{C_d} \left[D + A A'_{(OA)(mis)} \right] \quad (5-53)$$

If a' , d' , and τ are less than unity, the iteration method of Appendix A can be used to solve equation (5-49). The average float deflection angle averaged over a vibration cycle

is

$$\bar{\theta} = \frac{a'd'(k' - \tau\omega^2)}{2k' \left[\omega^2 + (k' - \tau\omega^2)^2 \right]} \quad (5-54)$$

From equations (5-52) and (5-53)

$$a'd' = \left(\frac{mL}{C_d} \right)^2 \left[AD + A^2 A'_{(OA)(mis)} - D^2 A'_{(OA)(mis)} - AD A'^2_{(OA)(mis)} \right] \quad (5-55)$$

If A and D are of the same order of magnitude and much greater than $A'_{(OA)(mis)}$, equation (5-55) becomes with very little error

$$a'd' \approx \left(\frac{mL}{C_d} \right)^2 AD \quad (5-56)$$

Substituting equations (5-50), (5-51), and (5-56) into equation (5-54) obtains

$$HG \bar{\theta} = \frac{(mL)^2 AD (HG - I\omega^2)}{2 \left[C_d^2 \omega^2 + (HG - I\omega^2)^2 \right]} \quad (5-57)$$

Equation (5-57) is the vibropendulum error with no unit misalignment (equation (4-9)). Therefore, the misalignment angle $(A_{(OA)(mis)})$ has a negligible effect in the vibropendulum torque.

By similar reasoning, it can be shown that for an input consisting of a vibration and an acceleration a unit misalignment will cause no significant increase in vibropendulum torque.

The analysis of this section assumed that the control member turned through a small angle during a cycle of vibration. For this case a misalignment between the LIX gyro input and control-member axes caused a negligible increase in vibropendulum

error. The vibropendulum error averaged over a revolution of the control member has been analyzed in Sections 5.4 and 5.5 of this chapter. The same analysis applies if the control-member axes are misaligned.

If the ratio of control-member angular velocity and vibration frequency are such that many revolutions of the control member occur during a cycle of vibration, the vibration input can be considered a constant acceleration for the interval for which the equations are solved. A cross-coupling error would occur. This case has been analyzed in Section 5.2 for no unit axes misaligned and in Section 5.3 for a misalignment between the LIX gyro input and control-member axes.

Misalignment of the gyro input and control-member axes increase the acceleration error only for the cases of constant acceleration input or for vibration frequencies such that many revolutions of the control member occur during a vibration cycle.

This chapter illustrated a major advantage of the gyro pendulum accelerometer over the pendulum accelerometer. If both units have the same elastic restraint, the gyro pendulum accelerometer will generally have much smaller cross-coupling, vibropendulum, and misalignment errors. The rotation of the control member reduces the acceleration error to one half the square of the error.

If an error in a pendulum accelerometer is one part in 10^5 , a gyro pendulum accelerometer with the same restraint will have an error of one half a part in 10^{10} as a result of the rotation of the control member.

CHAPTER 6

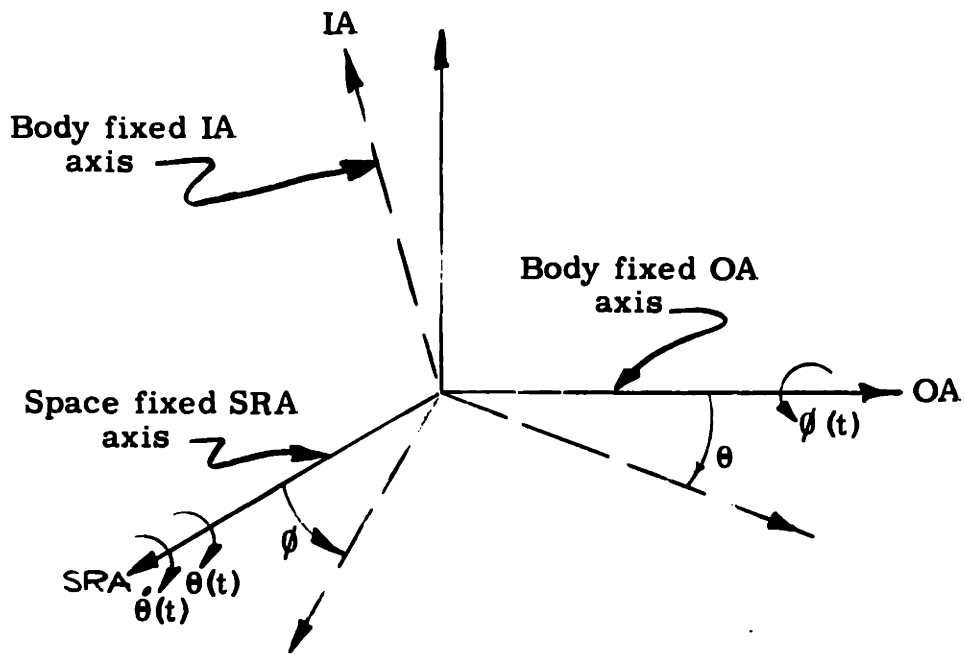
ERRORS DUE TO ANGULAR VIBRATION ABOUT TWO AXES IN THE PLANE OF THE LIX GYRO SPIN AND OUTPUT AXES

6.1 INTRODUCTION

It was shown in references 6, 15, and 16 that angular vibration applied about the spin and output axes of a gyro case may cause a gyro drift. This drift results when vibration applied about the gyro spin and output axes produces an average angular velocity component about the gyro input axis. This possibility is illustrated in Fig. 6-1 and discussed fully in reference 6.

The angular displacement about the output axis (ϕ) causes a component of the angular velocity that is being applied about the SRA axis ($\dot{\theta}$) to act about the gyro input axis. The angular velocity input to the gyro IA axis may result in a gyro drift. For the example which is illustrated in Fig. 6-1, an angular vibration about the OA axis equal to $b \sin \omega t$ and about the SRA axis equal to $a \cos \omega t$ caused an average angular velocity about the input axis equal to $\frac{ab}{2} \omega$.

This phenomenon has been called a coning effect and has been analyzed extensively for a gyro unit in references 6 and 15.



If $\theta = a \cos \omega t$

$\phi = b \sin \omega t$

$\dot{\phi} \theta = ab \omega \cos^2 \omega t$

$= \frac{ab}{2} \omega (1 + \cos 2 \omega t)$

$\dot{\phi} \theta =$ component of angular velocity along IA axis

Fig. 6-1

Drift resulting from angular vibration about gyro spin and output axes

The acceleration error of the linear integrating accelerometer when an angular vibration is applied about two axes in the plane of the LIX gyro spin and output axes is analyzed in this chapter.

Assume the linear integrating accelerometer is mounted in a gimbal in which two of the gimbal axes are initially aligned with the gyro output and spin reference axes. When angular vibration is applied about the gimbal axes, the component of angular vibration about the gyro output and spin reference axes continuously change as the control member of the LIX unit rotates. The coning error for the linear integrating accelerometer when it is subjected to an angular vibration about two gimbal axes is determined in this chapter.

The effect of LIX control-member rotation is included in the analysis. The coning error is determined for two performance functions of the control-member drive, a constant, and an integrator.

6.2 DEFINITIONS AND SYMBOLS

The following symbols and definitions have been used in the analysis of this chapter.

a, b, c , constants (radian)

E, F, Q, J, M, N, P , constants (radian)

$$A = a \cos A_{cm} + b \sin A_{cm} \quad (\text{radian})$$

$$B = b \cos A_{cm} - a \sin A_{cm} \quad (\text{radian})$$

$$C = c \cos A_{cm} \quad (\text{radian})$$

$$D = c \cos A_{cm} \quad (\text{radian})$$

$C_{d(OA)}$ = damping coefficient of the gyro unit between the float and case about the output axis
 $\left(\frac{\text{dyne-cm-sec}}{\text{radian}}\right)$

I_{OA} = inertia of gyro float about its output axis
 (gm-cm^2)

H = angular momentum of gyro wheel $(\text{gm-cm}^2/\text{sec})$

G = steady-state gain of control-member drive system (sec^{-1})

$$h = \frac{H}{C_{d(OA)}}$$

$$\tau = \frac{I_{OA}}{C_{d(OA)}}$$

$$k = \frac{HG}{C_{d(OA)}}$$

$A_{(I-C)SRA}$ = angular rotation of the case about a fixed axis which coincides with the gyro spin reference axis when $A_{(I-C)OA} = 0$ (radian)

$\theta = A_{(I-F)OA}$ = angular rotation of the gyro float about the output axis (radian)

$A_{(I-C)OA}$ = angular rotation of the gyro case about its output axis (radian)

ω = circular frequency of vibration input (rad/sec)

X or Y = gimbal axes about which angular vibration is applied. These axes are aligned with the gyro spin reference and output axes at $t = 0$

$A_{(I-G)}$ = angular rotation of the LIX unit about the gimbal axis (radian)

A_{cm} = angular rotation of LIX control-member shaft (radian)

ω_{cm} = angular velocity of LIX control-member shaft (radian/second)

A_e = average error in measured acceleration due to coning (cm/sec²)

$\bar{\theta}$ = average value of $A_{(I-F)OA}$ over a vibration period (radian)

$PF_{(cm)}$ = performance function of control-member drive relating ω_{cm} to $A_{(C-F)OA}$

T = largest time constant of control-member performance function (seconds)

mL = pendulosity of gyro float along its spin axis (gm-cm)

p = $\frac{d}{dt}$

6.3 COMPONENT OF ANGULAR VIBRATION ABOUT THE LIX GYRO OUTPUT AND SPIN REFERENCE AXES AS THE CONTROL MEMBER ROTATES

Consider the linear integrating accelerometer mounted in a gimbal in which the gyro spin reference and output axes are aligned with the X and Y gimbal axes at $t = 0$. As the control member rotates, the angle between the gyro axes and gimbal axes changes.

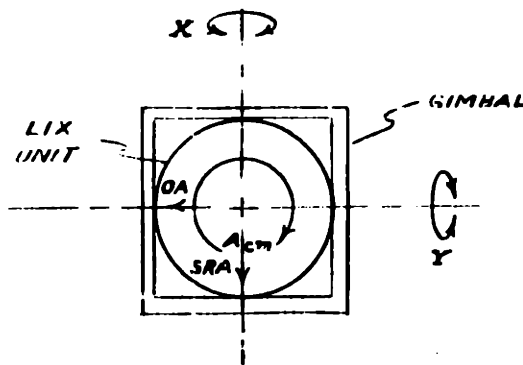


Fig. 6-2
LIX unit mounted in gimbal

For an angular vibration input to the gimbal axes of the form

$$A_{(I-G)X} = a \sin \omega t \quad (6-1)$$

$$A_{(I-G)Y} = b \sin \omega t + c \cos \omega t \quad (6-2)$$

The component of angular vibration about an axis that coincides with the spin reference axis when $A_{(I-C)OA} = 0$ is

$$A_{(I-C)SRA} = (a \sin \omega t) \cos A_{cm} + (b \sin \omega t + c \cos \omega t) \sin A_{cm} \quad (6-3)$$

The component of angular vibration about the LIX gyro output axis is

$$A_{(I-C)OA} = (b \sin \omega t + c \cos \omega t) \cos A_{cm} - (a \sin \omega t) \sin A_{cm} \quad (6-4)$$

Equation (6-3) and equation (6-4) are of the form

$$A_{(I-C)SRA} = A \sin \omega t + D \cos \omega t \quad (6-5)$$

$$A_{(I-C)OA} = B \sin \omega t + C \cos \omega t \quad (6-6)$$

where

$$A = a \cos A_{cm} + b \sin A_{cm} \quad (6-7)$$

$$B = b \cos A_{cm} - a \sin A_{cm} \quad (6-8)$$

$$C = c \cos A_{cm} \quad (6-9)$$

$$D = c \sin A_{cm} \quad (6-10)$$

6.4 CONING ERROR WHEN THE PERFORMANCE FUNCTION OF THE CONTROL-MEMBER DRIVE IS A CONSTANT GAIN

It will be shown in Chapter 7 that at low control-member frequencies the performance function relating gyro float angle to control-member angular velocity will be a constant (G). The coning errors for this case will be analyzed in this section.

For this analysis, it is assumed that the stiffness between the wheel and float about the gyro input and output axes are infinite. It is also assumed that there is no radial float motion about the input axis.

With the above two assumptions, the sum of the torques acting on the LIX gyro float becomes (as in reference 6)

$$HG(A_{(I-F)OA} - A_{(I-C)OA}) + C_{d(OA)} (\dot{A}_{(I-F)OA} - \dot{A}_{(I-C)OA}) + I_{OA} \ddot{A}_{(I-F)OA} = H \dot{A}_{(I-C)SRA} A_{(I-F)OA} \quad (6-11)$$

In equation (6-11), the elastic restraint about the output axis equals HG where

H = angular momentum of gyro wheel (gm-cm²/sec)

G = steady-state gain of control-member drive system

That the elastic restraint about the output axis equals HG can be verified by the following. The analysis is for the control-member performance function a constant or the control-member angular velocity (ω_{cm}) is given by

$$\omega_{cm} = GA_{(C-F)OA} \quad (6-12)$$

The torque on the float about the output axis ($M_{(OA)(cm)}$) due to the control-member rotation equals

$$M_{(OA)cm} = H \omega_{cm} = HG A_{(C-F)OA} \quad (6-13)$$

The gyro float therefore has an elastic restraint about its output axis equal to HG.

Dividing through by $C_{d(OA)}$ and rearranging terms, equation (6-11) becomes

$$\left(k - h \dot{A}_{(I-C)SRA} \right) \theta + \dot{\theta} + \tau \ddot{\theta} = \dot{A}_{(I-C)OA} + k A_{(I-C)OA} \quad (6-14)$$

where

$$k = \frac{HG}{C_{d(OA)}} \quad (6-15)$$

$$h = \frac{H}{C_{d(OA)}} \quad (6-16)$$

$$\tau = \frac{I_{OA}}{C_{d(OA)}} \quad (6-17)$$

and

$$\theta = A_{(I-F)OA} \quad (6-18)$$

With the angular vibration input of equations (6-5) and (6-6), equation (6-14) becomes

$$\begin{aligned} & [k - h (A \omega \cos \omega t - D \omega \sin \omega t)] \theta + \dot{\theta} + \tau \ddot{\theta} \\ & = B \omega \cos \omega t - C \omega \sin \omega t + k [B \sin \omega t + C \cos \omega t] \end{aligned} \quad (6-19)$$

If the control member turns through a small angle during a cycle of vibration, A, B, C, and D can be assumed constant in the solution of equation (6-19).

By a change of variables, equation (6-17) can be reduced to the standard Mathieu equation. As discussed by references 6, 7, and 8, there is no closed-form solution for the Mathieu equation or equation (6-19). If the constants h, A, B, C, D, and τ

are less than unity, the method of solution illustrated in reference 6 can be applied to solve equation (6-19). The constants for the LIX unit can be found in Chapter 6 of the Classified supplement of this report.

The solution of equation (6-19) is of the form

$$\theta = \theta_1 + \theta_3 + \theta_5 + \dots + \theta_{(2m-1)} + \theta_{2m} \quad (6-20)$$

where

$$\begin{aligned} k\theta_1 + \dot{\theta}_1 + \tau\ddot{\theta}_1 &= B\omega \cos \omega t - C\omega \sin \omega t \\ &+ k(B \sin \omega t + C \cos \omega t) \end{aligned} \quad (6-21)$$

$$k\theta_3 + \dot{\theta}_3 + \tau\ddot{\theta}_3 = h(A\omega \cos \omega t - D\omega \sin \omega t)\theta_1 \quad (6-22)$$

$$k\theta_5 + \dot{\theta}_5 + \tau\ddot{\theta}_5 = h(A\omega \cos \omega t - D\omega \sin \omega t)\theta_3 \quad (6-23)$$

Consecutively to

$$\begin{aligned} k\theta_{(2m-1)} + \dot{\theta}_{(2m-1)} + \tau\ddot{\theta}_{(2m-1)} \\ = h(A\omega \cos \omega t - D\omega \sin \omega t)\theta_{(2m-3)} \end{aligned} \quad (6-24)$$

$$\begin{aligned} [k - h(A\omega \cos \omega t - D\omega \sin \omega t)]\theta_{2m} + \dot{\theta}_{(2m)} + \tau\ddot{\theta}_{2m} \\ = h(A\omega \cos \omega t - D\omega \sin \omega t)\theta_{(2m-1)} \end{aligned} \quad (6-25)$$

The solution of equation (6-21) is of the form

$$\theta_1 = E \sin \omega t + F \cos \omega t \quad (6-26)$$

where

$$E = \frac{B \left[1 + \left(\frac{k}{\omega} \right)^2 - \tau k \right] + \tau \omega C}{1 + \left[\frac{k}{\omega} - \tau \omega \right]^2} \quad (6-27)$$

$$F = \frac{C \left[1 + \left(\frac{k}{\omega} \right)^2 - \tau k \right] - \tau \omega B}{1 + \left[\frac{k}{\omega} - \tau \omega \right]^2} \quad (6-28)$$

Substituting equation (6-26) into equation (6-22) yields

$$k\theta_3 + \dot{\theta}_3 + \tau\ddot{\theta}_3 = h \left[\frac{A\omega F - D\omega E}{2} + \left(\frac{A\omega E - D\omega F}{2} \right) \sin 2\omega t + \left(\frac{A\omega F + D\omega E}{2} \right) \cos 2\omega t \right] \quad (6-29)$$

The solution of this equation is

$$\theta_3 = Q + J \sin 2\omega t + M \cos 2\omega t \quad (6-30)$$

where

$$Q = \frac{h}{k} \left[\frac{A\omega F - D\omega E}{2} \right] \quad (6-31)$$

The solution of equations (6-23) to (6-24) can be obtained in a similar manner. For A, B, C, and D of the same order of magnitude and much less than unity, each successive term in equation (6-20) grows smaller by a factor of A. If θ_1 is of the order of magnitude of unity, θ_3 will be of the order of magnitude of A and $\theta_{(2m+1)}$ will be of the order of magnitude of A^m . For

small values of A, B, C, and D, sufficient accuracy is obtained by taking

$$\theta = \theta_1 + \theta_3 + \theta_{2m} \quad (6-32)$$

The stability and convergence to zero of θ_{2m} can be shown by the method of Appendix A. Therefore, with little error*

$$\theta = \theta_1 + \theta_3 \quad (6-33)$$

Substituting the values of θ_1 and θ_3 from equations (6-26) and (6-30) yields

$$\theta = E \sin \omega t + F \cos \omega t + Q + J \sin 2 \omega t + M \cos 2 \omega t \quad (6-34)$$

Combining equations (6-15), (6-16), and (6-31), the float deflection angle averaged over a cycle of vibration is equal to

$$\bar{\theta} = Q = \frac{\omega}{2G} [AF - DE] \quad (6-35)$$

Substituting the value of E and F from equations (6-27) and (6-28) yields

$$\theta = \frac{\omega}{2G} \left\{ \frac{AC \left[1 + \left(\frac{k}{\omega} \right)^2 - \tau k \right] - AB\tau\omega}{1 + \left(\frac{k}{\omega} - \tau\omega \right)^2} - \frac{BD \left[1 + \left(\frac{k}{\omega} \right)^2 - \tau k \right] + CD\tau\omega}{1 + \left(\frac{k}{\omega} - \tau\omega \right)^2} \right\} \quad (6-36)$$

*The accuracy with which equation (6-33) approximates equation (6-20) for the LIX unit is given in Chapter 6 of the classified supplement.

Substituting the values of A, B, C, and D from equations (6-7) through (6-10) into equation (6-36) obtains

$$\bar{\theta} = \frac{\omega}{2G} \left\{ \frac{ac \left[1 + \left(\frac{k}{\omega} \right)^2 - \tau k \right] - \tau \omega \left[ab \cos 2 A_{cm} + \frac{b^2 - a^2 + c^2}{2} \sin 2 A_{cm} \right]}{1 + \left(\frac{k}{\omega} - \tau \omega \right)^2} \right\}$$

(6-37)

The float deflection angle averaged over a period of control-member rotation is

$$\theta_{av} = \frac{\omega ac}{2G} \left[\frac{1 + \left(\frac{k}{\omega} \right)^2 - \tau k}{1 + \left(\frac{k}{\omega} - \tau \omega \right)^2} \right]$$

(6-38)

The average error in LIX measured acceleration (A_e) due to applying the angular vibration of Section 6.3 is

$$A_e = \frac{H\omega ac}{2mL} \left[\frac{1 + \left(\frac{k}{\omega} \right)^2 - \tau k}{1 + \left(\frac{k}{\omega} - \tau \omega \right)^2} \right]$$

(6-39)

The variation of acceleration error with control-member rotation is plotted in Fig. 6-3.

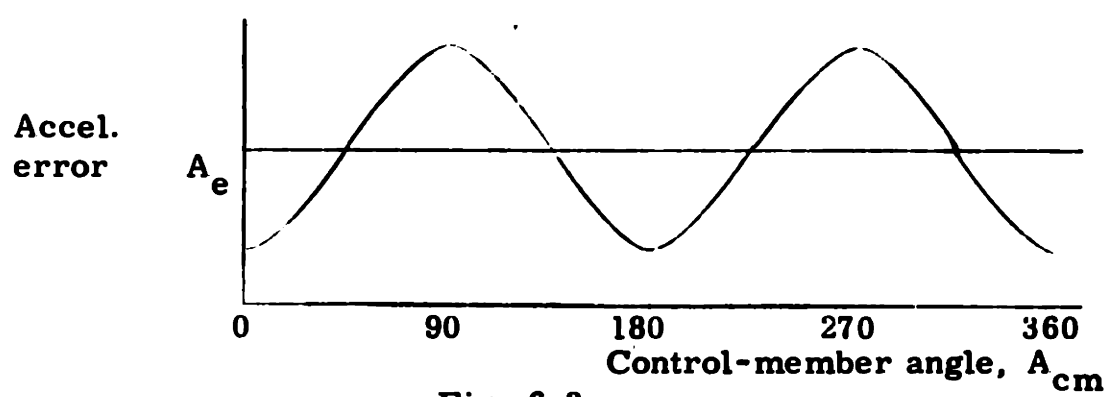


Fig. 6-3

Acceleration error vs. control-member angle

From equation (6-37), the amplitude of the sinusoidal portion of the acceleration error curve is equal to

$$- \tau \omega \left[(\epsilon b)^2 + \left(\frac{b^2 - a^2 + c^2}{2} \right)^2 \right]^{1/2} \quad (6-40)$$

The acceleration error would not change with control-member rotation if $b = 0$ and $a = c$ (as verified from equation (6-40)). The acceleration error would be given by equation (6-39) and would be constant with control-member rotation for this case.

6.5 CONING ERROR WHEN THE PERFORMANCE FUNCTION OF THE CONTROL-MEMBER DRIVE IS AN INTEGRATOR

Chapter 7 shows that at some range of control-member angular frequencies the control-member angular velocity will be proportional to the integral of gyro float angle.

The coning error for the frequency range in which the performance function of the control-member drive is an integrator is determined in this section.

Assuming infinite stiffness between the wheel and the float about the gyro input and output axis and assuming there is no float motion about the gyro input axis, the sum of the torques acting on the LIX gyro float is given by

$$\begin{aligned} \text{HG} \int \left(A_{(I-F)OA} - A_{(I-C)OA} \right) dt + C_{d(OA)} \left(\dot{A}_{(I-F)OA} - \dot{A}_{(I-C)OA} \right) \\ + I_{OA} \ddot{A}_{(I-F)OA} = H \dot{A}_{(I-C)SRA} A_{(I-F)OA} \end{aligned} \quad (6-41)$$

The constants of equation (6-41) have been defined in Section 6. 2.

Differentiating equation (6-41), dividing through by $C_{d(OA)}$ and rearranging terms yield

$$\begin{aligned} & \left(k - h\ddot{A}_{(I-C)SRA} \right) \theta - h\dot{A}_{(I-C)SRA} \dot{\theta} + \ddot{\theta} + \tau\ddot{\theta} \\ & = kA_{(I-C)OA} + \ddot{A}_{(I-C)OA} \end{aligned} \quad (6-42)$$

where

$$k = \frac{HG}{C_{d(OA)}} \quad (6-15) \text{ repeated}$$

$$h = \frac{H}{C_{d(OA)}} \quad (6-16) \text{ repeated}$$

$$\tau = \frac{I_{OA}}{C_{d(OA)}} \quad (6-17) \text{ repeated}$$

$$\theta = A_{(I-F)OA} \quad (6-18) \text{ repeated}$$

Substituting the values of $A_{(I-C)SRA}$ and $A_{(I-C)OA}$ from equations (6-5) and (6-6) into equation (6-42) obtains

$$\begin{aligned} & \left(k + hA\omega^2 \sin \omega t + hD\omega^2 \cos \omega t \right) \theta - h(A\omega \cos \omega t - D\omega \sin \omega t) \dot{\theta} + \ddot{\theta} + \tau\ddot{\theta} \\ & = k(B \sin \omega t + C \cos \omega t) - B\omega^2 \sin \omega t - C\omega^2 \cos \omega t \end{aligned} \quad (6-43)$$

Using the iteration method of Appendix A, the solution of equation (6-43) may be expressed as the series

$$\theta = \theta_1 + \theta_3 + \theta_5 + \dots + \theta_{(2m-1)} + \theta_{(2m)} \quad (6-44)$$

where

$$k\theta_1 + \ddot{\theta}_1 + \tau\ddot{\theta}_1 = k B \sin \omega t + k C \cos \omega t - B \omega^2 \sin \omega t - C \omega^2 \cos \omega t \quad (6-45)$$

$$k\theta_3 + \ddot{\theta}_3 + \tau\ddot{\theta}_3 = (-hA\omega^2 \sin \omega t - hD\omega^2 \cos \omega t)\theta_1 + (hA\omega \cos \omega t - hD\omega \sin \omega t) \dot{\theta}_1 \quad (6-46)$$

$$k\theta_5 + \ddot{\theta}_5 + \tau\ddot{\theta}_5 = (-hA\omega^2 \sin \omega t - hD\omega^2 \cos \omega t)\theta_3 + (hA\omega \cos \omega t - hD\omega \sin \omega t) \dot{\theta}_3 \quad (6-47)$$

Consecutively to

$$k\theta_{(2m-1)} + \ddot{\theta}_{(2m-1)} + \tau\ddot{\theta}_{(2m-1)} = (-hA\omega^2 \sin \omega t - hD\omega^2 \cos \omega t)\theta_{(2m-3)} + (hA\omega \cos \omega t - hD\omega \sin \omega t)\dot{\theta}_{(2m-3)} \quad (6-48)$$

$$(k + hA\omega^2 \sin \omega t + hD\omega^2 \cos \omega t)\theta_{2m} - (hA\omega \cos \omega t - hD\omega \sin \omega t)\dot{\theta}_{2m} + \ddot{\theta}_{2m} + \tau\ddot{\theta}_{2m} = - (hA\omega^2 \sin \omega t + hD\omega^2 \cos \omega t)\theta_{(2m-1)} + (hA\omega \cos \omega t - hD\omega \sin \omega t)\dot{\theta}_{(2m-1)} \quad (6-49)$$

The solution of equation (6-45) is of the form

$$\theta_1 = J \sin \omega t + M \cos \omega t \quad (6-50)$$

Substituting equation (6-50) into equation (6-46)

yields

$$k\theta_3 + \ddot{\theta}_3 + \tau\ddot{\theta}_3 = h\omega^2 [(AJ - DM) \cos 2\omega t - (AM + DJ) \sin 2\omega t] \quad (6-51)$$

The solution of equation (6-51) is

$$\theta_3 = N \sin 2 \omega t + P \cos 2 \omega t \quad (6-52)$$

The solutions of equations (6-47) to (6-48) can be obtained in a similar manner.

Successive terms in the solution of θ will be harmonics of the vibration frequency.

The convergence and stability of the solution of θ can be shown by the method of Appendix A.

The past analysis has shown that the gyro float angle for this angular vibration input is periodic. Therefore, there is no average float deflection angle or acceleration error over a vibrational cycle when the control-member performance function is an integrator.

In Chapter 4, it was shown that with the control-member performance function an integrator there was no cross-coupling or vibropendulum error under a linear acceleration. Therefore, an integrator is the desired control-member drive performance function, since it prevents all cross-coupling vibropendulum and coning errors if the unit axes are perfectly aligned.

The stability of the LIX loop with an integrator added to the control-member drive loop is discussed in Section 7.5 of Chapter 7.

A conservative error analysis is obtained for the LIX unit by assuming the performance function of the control-member

drive is a constant since this is the case that will obtain cross-coupling, vibropendulum, and coning errors.

If an integrator is not added to the control-member drive system, at low frequencies the performance function of the control-member drive is of the form

$$PF_{(cm)} = \frac{G}{1 + T p} \quad (6-53)$$

At very low control-member frequencies ($\omega_{cm} \ll \frac{1}{T}$ rad/sec), the control-member performance function will be a constant G . At higher control member frequencies ($\omega_{cm} \gg \frac{1}{T}$ rad/sec), the control-member performance function is an integrator. Therefore, the largest cross-coupling, vibropendulum, and coning errors occur for control-member angular frequencies less than $\frac{1}{T}$ where T is the largest time constant of the control-member drive performance function.

CHAPTER 7

LIX LOOP DYNAMICS

7.1 INTRODUCTION

The performance functions* for the pendulous integrating gyro and control-member drive are determined. These performance functions are combined with those of the other loop components, and a LIX loop performance function is obtained. The LIX performance function is the ratio of control-member angular velocity to input acceleration.

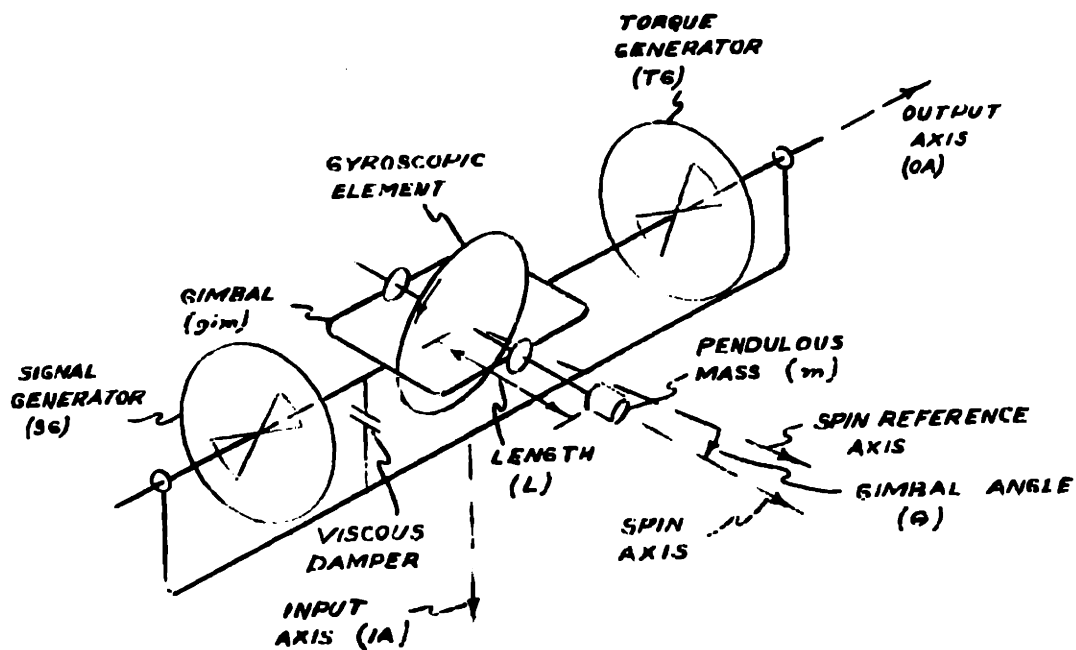
As discussed in Chapters 4 and 6, the cross-coupling, vibropendulum, and coning errors would be eliminated if the performance function of the control-member drive system is a perfect integrator at all control-member frequencies. For this reason, the LIX loop with an integrator added to the control-member drive is also discussed.

7.2 PERFORMANCE FUNCTION OF AN IDEAL PENDULOUS INTEGRATING GYRO UNIT

The sum of the torques acting about the output axis of the gyro for small float deflection angles is

$$I\ddot{\theta} + C_d\dot{\theta} + H\omega_{cm} = mL\ddot{a} \quad (7-1)$$

*A performance function is defined as the ratio of the Laplace transformation of the output of a unit to the Laplace transformation of its input.



Pendulous integrating gyro

Fig. 7-1

where

- I = moment of inertia of gyro float about its output axis (gm-cm^2)
- C_d = damping coefficient between the float and case about the output axis (dyne-cm-sec./rad)
- H = angular momentum of gyro wheel (gm-cm^2)
- ω_{cm} = angular velocity about gyro input axis (rad/sec)
- mL = float pendulosity along gyro spin axis (gm-cm)
- a = input linear acceleration along the gyro input axis of the gyro case with respect to inertial space (cm/sec^2)
- θ = float deflection angle measured about the output axis from the position under no input acceleration to the position under the applied acceleration.

Dividing equation through by H yields

$$\frac{I}{H} \ddot{\theta} + \frac{C_d}{H} \dot{\theta} + \omega_{cm} = \frac{mLa}{H} \quad (7-2)$$

A block diagram for the pendulous integrating gyro is shown in Fig. 7-2.

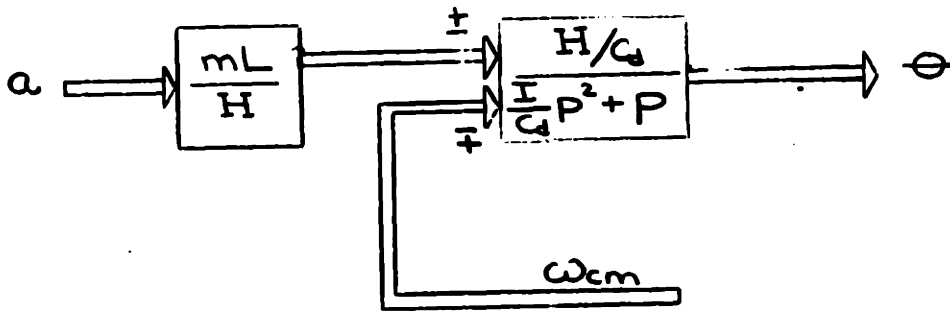


Fig. 7-2

Block diagram of pendulous integrating gyro

7.3 PERFORMANCE FUNCTION OF LIX DRIVE MOTOR

A DC torque motor having a constant field excitation is shown in Fig. 7-3.

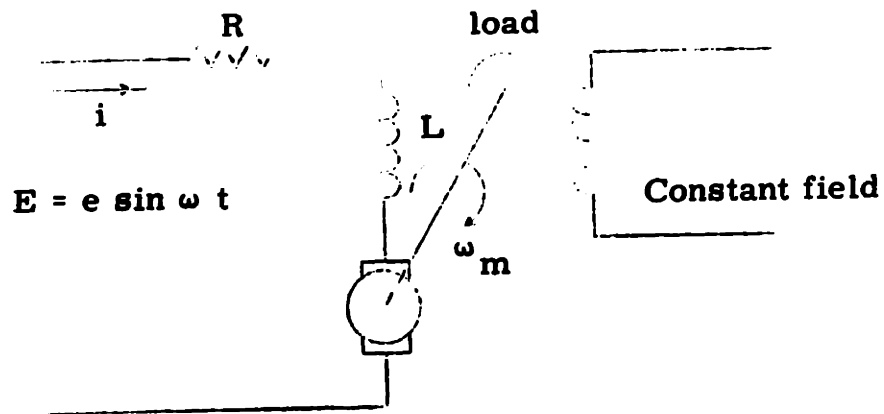


Fig. 7-3

DC torque motor

The constants for the motor are defined as follows

E = applied voltage (volts)

R = armature circuit resistance (ohms)

L = inductance of armature winding (henries)

i = armature current (amps)

K_e = back emf constant of motor (volts / radian / sec)

K_t = torque constant of motor (dyn-cm / amp)

ω_m = angular velocity of motor shaft (rad / sec)

J = motor and load inertia (gm-cm²)

$PF_m = \frac{\omega_m}{E}$ = performance function of motor

p = Laplace transform operator

The voltage input is equal to the drop across the motor armature plus the back emf

$$E = Ri + L \frac{di}{dt} + K_e \omega \quad (7-3)$$

The torque accelerating the motor and load inertia is proportional to the motor current flowing (assuming no damping or elastic restraint on the motor shaft)

$$J \frac{d\omega}{dt} = K_t i \quad (7-4)$$

Taking the Laplace transformation of equations (7-3) and (7-4), combining and rearranging terms (assuming the initial conditions are equal to zero) yields

$$PF_m = \frac{\omega_m}{E} = \frac{K_t}{JL p^2 + J R p + K_e K_t} \quad (7-5)$$

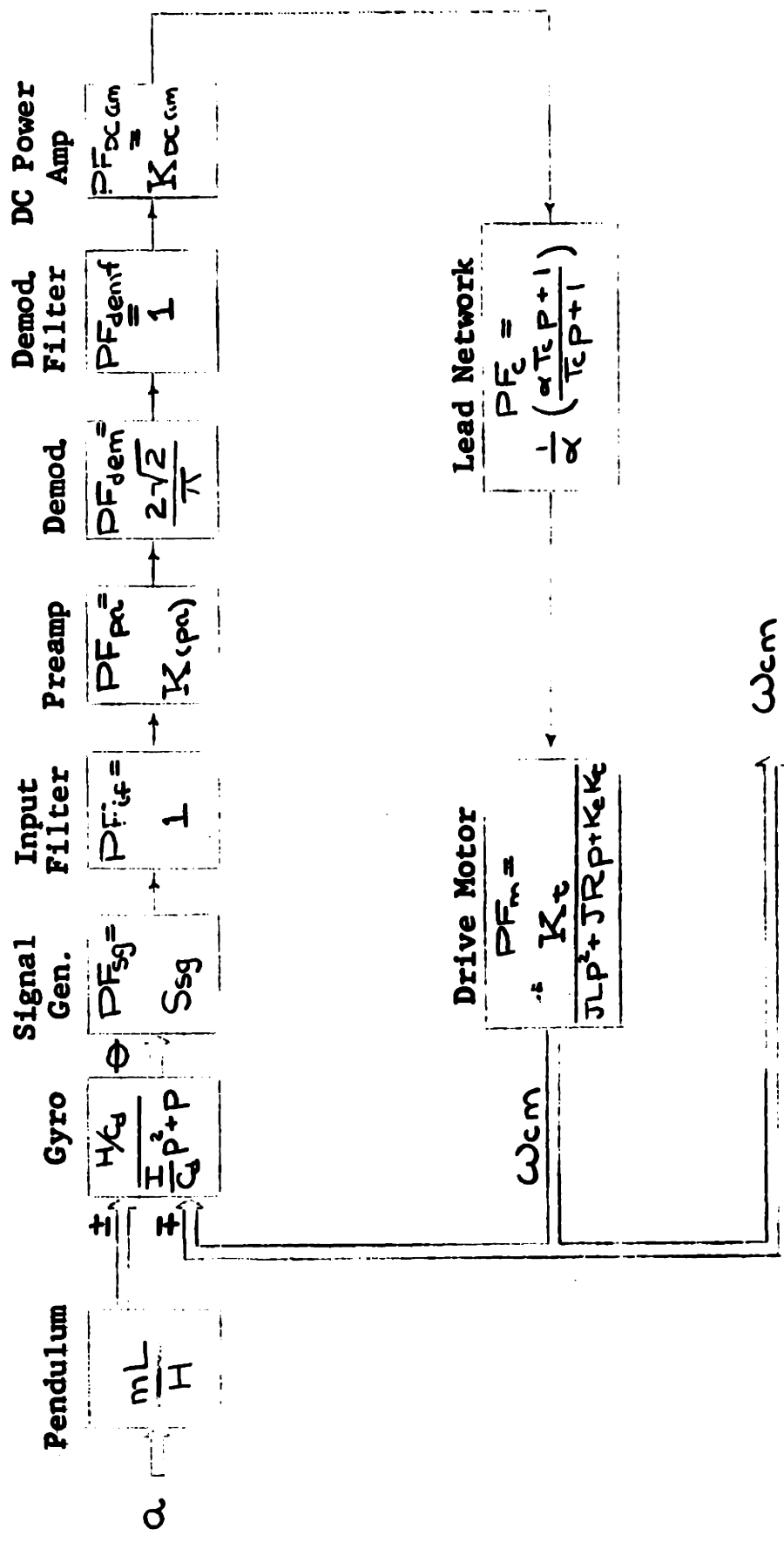
7.4 PERFORMANCE FUNCTION OF LIX UNIT

The block diagram of the linear integrating accelerometer is shown in Fig. 7-4.

The performance function of the pendulous gyro unit was determined in Section 7.2 and of the drive motor in Section 7.3.

The performance function of the other components is

Signal generator	$PF_{sg} = S_{sg} \text{ mv/mr}$
Input filter	PF_{if} assumed equal to 1. This is reasonable since filter can be designed to give very little phase shift in range of excitation frequency. If this assumption is not true, the performance function of this element should be added to the loop.
Preamplifier	$PF_{(pa)} = K_{(pa)} \text{ volts/volt}$
Full-wave demodulator	$PF_{(dem)} = \frac{2\sqrt{2}}{\pi} \text{ volts dc/volts rms AC}$ $= 0.9$
Demodulator filter	$PF_{(dem f)}$ assumed = 1 since there is negligible phase shift at modulation frequency.
DC power amplifier	$PF_{(DC am)} = K_{(DC)(am)} \text{ volts/volt}$
Lead compensation (reference 10)	$PF_c = \frac{1}{\alpha} \left(\frac{\alpha T_c p + 1}{T_c p + 1} \right)$



Block Diagram of Linear Integrating Accelerometer

Fig. 7-4

The LIX unit is thus represented as a unity feedback system by Fig. 7-5

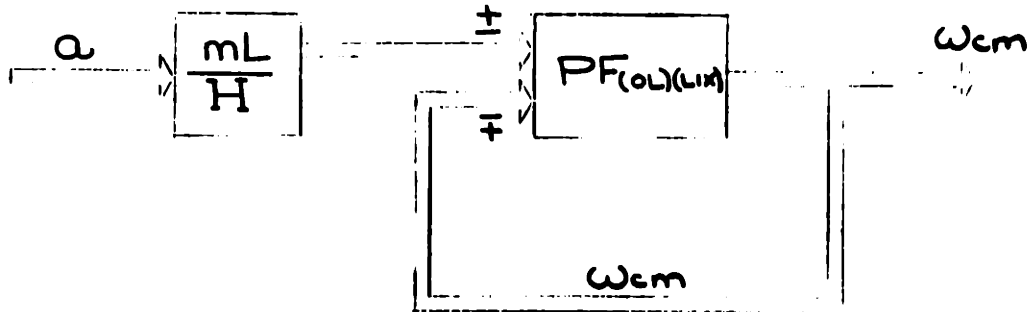


Fig. 7-5

Block diagram of LIX unit

The open-loop performance function, $PF_{(OL)(LIX)}$, is the product of the performance functions of the loop components (illustrated in Fig. 7-4). Its value is given by

$$PF_{(OL)(LIX)} = \frac{\left(\frac{H}{C_d}\right) (S_{sg}) (K_{(pa)}) (0.9)K_{(DC)(am)} (\alpha T_c p + 1) K_t}{\left(\frac{I}{C_d} p^2 + p\right) (\alpha) (T_c p + 1) (JLp^2 + JRp + K_e K_t)}$$

(7-6)

Referring to equation (7-6) and Fig. 7-5, the closed-loop performance function for the LIX unit is obtained by

$$PF_{(LIX)} = \frac{\omega_{cm}}{a} = \frac{\frac{mL}{H} PF_{(OL)(LIX)}}{1 + PF_{(OL)(LIX)}} \quad (7-7)$$

Another form for the block diagram of the LIX unit is shown in Fig. 7-6.

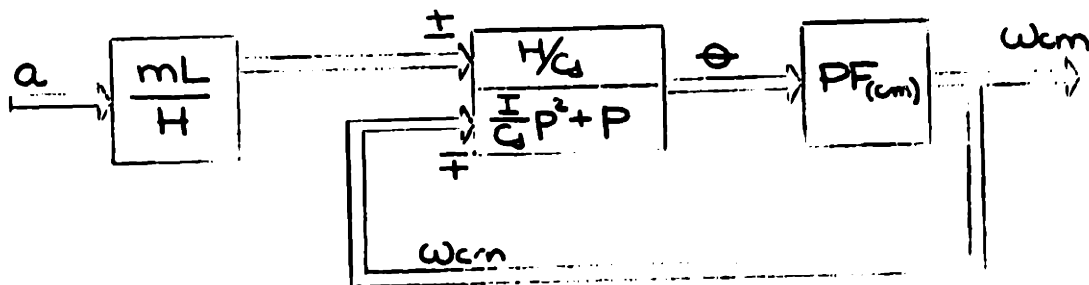


Fig. 7-6

Block diagram of LIX unit

Where the performance function of the control-member drive is

$$PF_{(cm)} = \frac{\omega_{cm}}{\theta} = \frac{S_{(sg)} K_{(pa)} (0.9) K_{(DC)}(am) (\alpha T_e p + 1) K_t}{\alpha (T_c p + 1) (JLp^2 + JRp + K_e K_t)}$$

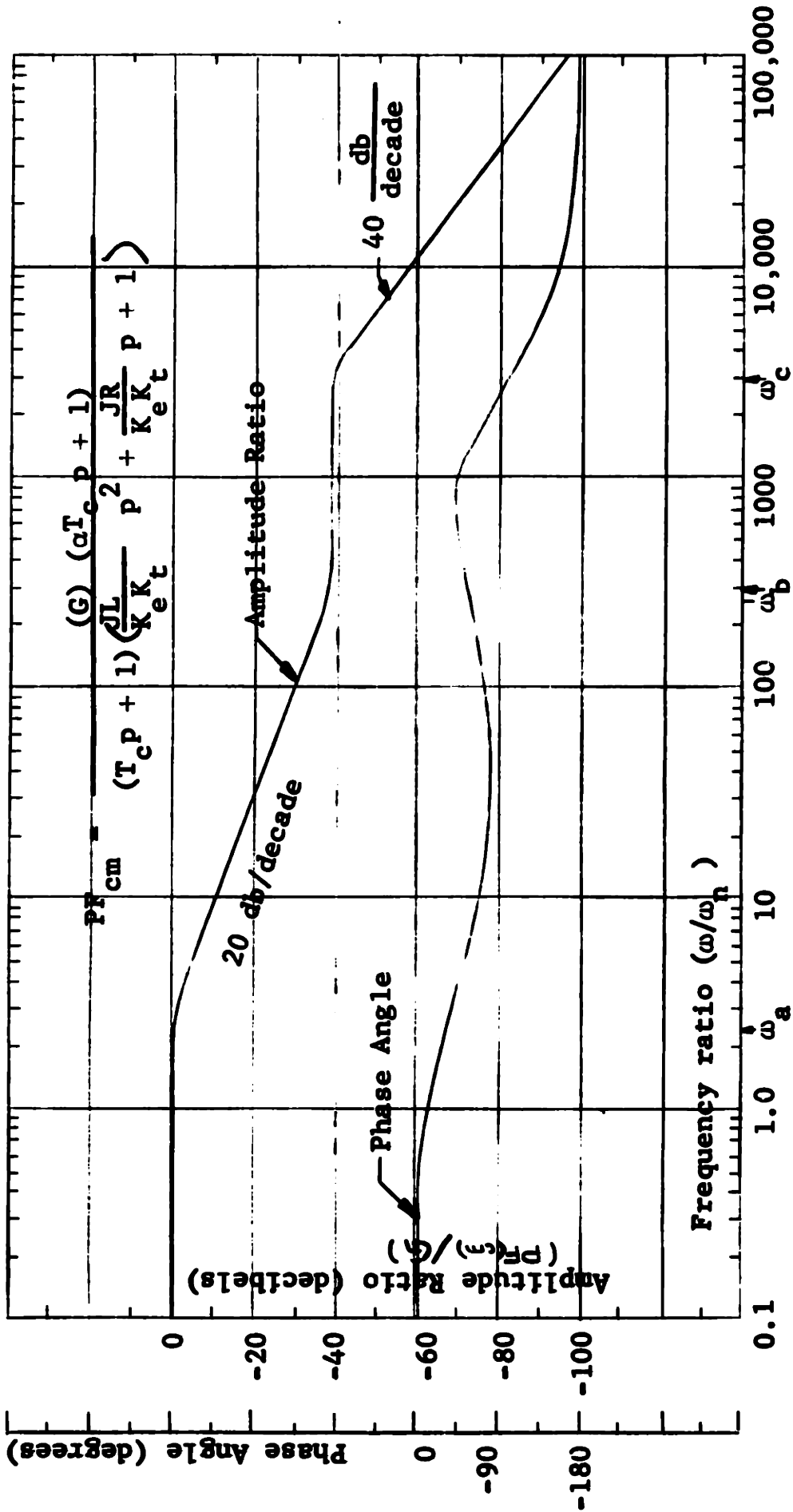
(7-8)

The amplitude and phase of the performance function of the control-member drive for a typical gyro pendulum accelerometer is plotted in Fig. 7-7.

At low-control-member frequencies, the performance function of the control-member drive is a constant (defined as G in Chapters 4, 5, and 6) given by

$$G = \frac{(0.9) (S_{sg}) K_{(pa)} K_{(DC)}(am)}{\alpha K_e}$$

(7-9)



Control Member Drive Performance Function
vs. Frequency Ratio
for Typical Gyro Pendulum Accelerometer

As illustrated in Fig. 7-7, at control-member frequencies less than ω_a radians/second and between ω_b and ω_c radians/second, the control-member drive performance function is a constant.

A method to determine the magnitude of cross-coupling, vibropendulum, and coning error that would occur in this frequency range is presented in Chapters 4 and 6.

At control-member frequencies between ω_a and ω_b radians/second and greater than ω_c radians/second, the control-member drive performance function is an integrator. There will be no cross-coupling, vibropendulum, or coning error for a perfectly aligned gyro pendulum accelerometer operating in this control-member frequency range.

7.5 CONTROL-MEMBER DRIVE PERFORMANCE FUNCTION WITH AN INTEGRATOR

As shown in Chapters 4 and 6, an ideal integrator is the desired performance function of the control-member drive system.

Adding an integrator to the control-member drive performance function plotted in Fig. 7-7 will make the performance function an integrator at all control-member frequencies. The lead network is used to stabilize the loop.

This system will have no cross-coupling, vibropendulum, or coning errors for a perfectly aligned unit. Therefore, this is the recommended loop to be used with the LIX unit.

It is suggested that, with an integrator added to the control-member drive loop, further study be made to determine what

changes in LIX unit parameters should be made to obtain an optimum LIX loop. An optimum loop is one in which the control-member drive performance function is an integrator at all control-member frequencies, and the loop has maximum stability at all control-member frequencies.

CHAPTER 8

CONCLUSIONS AND RECOMMENDATIONS

8.1 CONCLUSIONS

As a result of this investigation, it is concluded that pendulum accelerometers and gyro pendulum accelerometers will experience errors in the measurement of true acceleration.

For an input consisting of a translation steady-state or vibratory acceleration

- a. The magnitude of these errors are directly proportional to the pendulosity and to the component of the input perpendicular to the pendulum sensitive axis. The error is inversely proportional to the pendulum restraint.
- b. The error in the measurement of acceleration is directly proportional to misalignment angle between the LIX gyro input and control-member axes. Therefore, the degree of precision required in alignment of the unit axes is dictated by the accuracy requirement for the instrument.

- c. If the dynamics of the loop are adjusted so that the restraint torque is proportional to the integral of the float deflection angle, there will be no acceleration error averaged over a vibration cycle due to translational steady-state acceleration and a translational or an angular vibratory acceleration.
- d. The acceleration errors averaged over complete revolutions of the control member, due to the translational steady-state and vibratory accelerations and due to the misalignments between the pendulous gyro's input and control-member axes, are equal to one half the square of the dimensionless error that occurs for the condition of a nonrotating control member. Since the dimensionless errors are less than unity, the acceleration errors will generally be reduced by the rotation of the control member. For example, if an acceleration error with a stationary control member is one part in 10^5 , the error averaged over a rotation of the control member will be $1/2$ part in 10^{10} . Therefore, gyro pendulum accelerometers will generally have much smaller acceleration errors than pendulum accelerometers of equal elastic restraint.

8.2 RECOMMENDATIONS

It is recommended that

- a. An integrator be added to the control-member drive loop to make the performance function of the

control-member drive an integrator at all control-member frequencies. This will eliminate acceleration errors caused by translation steady-state acceleration and caused by translation or angular vibratory acceleration.

- b. Further studies be made to determine the most stable loop for which the control-member performance function is an integrator at all control-member frequencies.
- c. Linear and angular vibration tests be conducted on a LIX accelerometer to verify the theoretical results of this thesis.

APPENDIX A

VIBROPENDULOUS AND CROSS-COUPPLING TORQUE FOR PENDULUM HAVING ELASTIC RESTRAINT AND DAMPING

A.1 EQUATION OF MOTION OF A PENDULUM SUBJECTED TO TRANSLATIONAL ACCELERATION

Consider a pendulum as shown in Fig. A-1 having elastic restraint (exerting a torque proportional to angular displacement) and damping (offering a resistance proportional to angular velocity). The equation of motion for the pendulum when it is subjected to translational accelerations is given by

$$I\ddot{\theta} + C\dot{\theta} + (K - mL\ddot{Y})\theta = mL\ddot{X} \tag{A-1}$$

where

I = moment of inertia about pendulum pivot (gm-cm²)

C = damping coefficient of pendulum ($\frac{\text{dyne-cm-sec}}{\text{radian}}$)

K = rotational stiffness of pendulum ($\frac{\text{dyne-cm}}{\text{radian}}$)

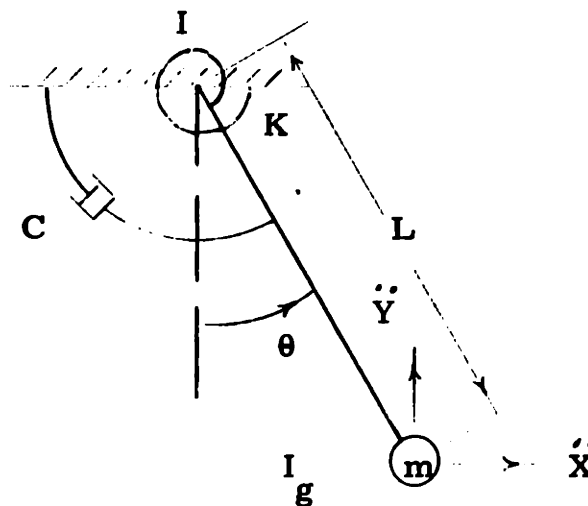
m = mass of pendulum (grams)

L = length of pendulum arm (cm)

θ = angle measured from the pendulum position under no input acceleration to the pendulum position under the applied input

\ddot{X} = acceleration of pendulum pivot in "X" direction
(cm/sec²)

\ddot{Y} = acceleration of pendulum pivot in "Y" direction
(cm/sec²)



$$\Sigma \text{ torques} - I\ddot{\theta} = 0$$

$$-K\theta - C\dot{\theta} + mL(\ddot{Y} \sin \theta) + mL(\ddot{X} \cos \theta) - I\ddot{\theta} = 0$$

where

$$I = I_g + mL^2$$

For small pendulum deflections

$$\sin \theta \approx \theta$$

$$\cos \theta \approx 1$$

The equation of motion for the pendulum becomes

$$I\ddot{\theta} + C\dot{\theta} + (K - mL\ddot{Y})\theta = mL\ddot{X}$$

(A-1)
repeated

Fig. A-1

Restrained pendulum subjected to translational acceleration

A. 2 **PENDULUM SUBJECTED TO A CONSTANT AND SINUSOIDAL ACCELERATION AT AN ANGLE TO THE PENDULUM SENSITIVE AXIS**

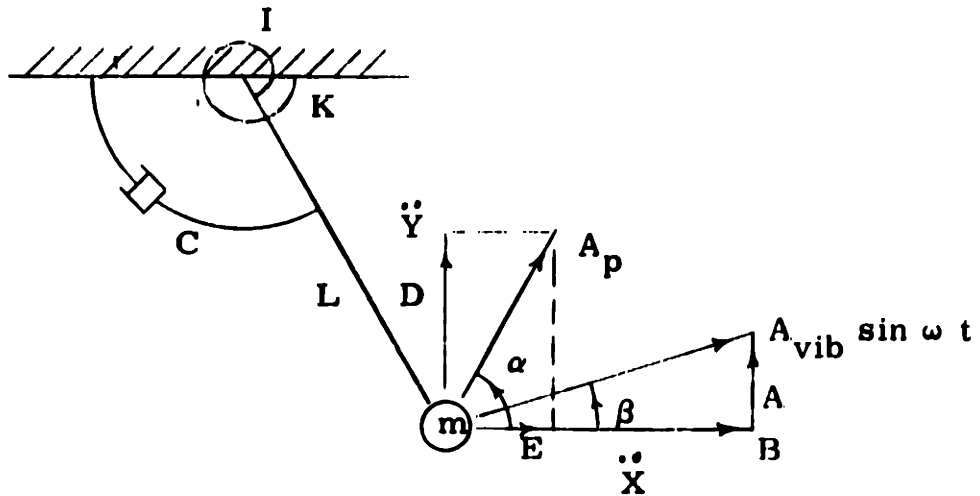


Fig. A-2

Pendulum subjected to a constant and sinusoidal acceleration

If the pendulum is subjected to a constant acceleration A_p at some angle α and a vibratory acceleration $A_{vib} \sin \omega t$ at some angle β to the pendulum axis as shown above, the acceleration input may be represented as

$$\begin{aligned} \ddot{Y} &= A \sin \omega t + D \\ \ddot{X} &= B \sin \omega t + E \end{aligned} \tag{A-2}$$

where

$$\begin{aligned} A &= A_{vib} \sin \beta \\ B &= A_{vib} \cos \beta \\ D &= A_p \sin \alpha \\ E &= A_p \cos \alpha \end{aligned} \tag{A-3}$$

For this acceleration input, equation (A-1) becomes

$$\tau \ddot{\theta} + \dot{\theta} + (k - a \sin \omega t) \theta = b \sin \omega t + e \tag{A-4}$$

where

$$\begin{aligned} \tau &= \frac{I}{C} & k &= \frac{K - mL D}{C} \\ a &= \frac{mLA}{C} & b &= \frac{mLB}{C} \\ e &= \frac{mLE}{C} & & \end{aligned} \quad (A-5)$$

By a change of variables, equation (A-4) can be reduced to the standard Mathieu equation. As discussed in references 6, 7, and 8, there is no closed-form solution for the Mathieu equation or equation (A-4). If the constants a , b , e , and τ are less than unity, the method of solution illustrated in reference 6 can be used to solve equation (A-4). Since the pendulum instruments considered in this analysis are low pendulosity highly overdamped units, the constants will be small.*

The solution of equation (A-3) is given by the series

$$\theta = \theta_1 + \theta_3 + \theta_5 + \dots + \theta_{(2m-1)} + \theta_{2m} \quad (A-6)$$

where

$$\tau \ddot{\theta}_1 + \dot{\theta}_1 + k\theta_1 = b \sin \omega t + e \quad (A-7)$$

$$\tau \ddot{\theta}_3 + \dot{\theta}_3 + k\theta_3 = (a \sin \omega t) \theta_1 \quad (A-8)$$

$$\tau \ddot{\theta}_5 + \dot{\theta}_5 + k\theta_5 = (a \sin \omega t) \theta_3 \quad (A-9)$$

*Values of a , b , e , and τ can be found in Appendix A of the classified supplement.

Consecutively to

$$\tau \ddot{\theta}_{(2m-1)} + \dot{\theta}_{(2m-1)} + k\theta_{(2m-1)} = (a \sin \omega t) \theta_{(2m-3)} \quad (\text{A-10})$$

$$\tau \ddot{\theta}_{2m} + \dot{\theta}_{2m} + (k - a \sin \omega t) \theta_{2m} = (a \sin \omega t) \theta_{(2m-1)} \quad (\text{A-11})$$

The solution of equation (A-7) is of the form

$$\theta_1 = F \sin \omega t + G \cos \omega t + J \quad (\text{A-12})$$

where

$$F = \frac{(k - \tau\omega^2) b}{\omega^2 + (k - \tau\omega^2)^2} \quad (\text{A-13})$$

$$G = \frac{-b\omega}{\omega^2 + (k - \tau\omega^2)^2} \quad (\text{A-14})$$

$$J = \frac{e}{k} \quad (\text{A-15})$$

Substitution of equation (A-12) into (A-8) yields

$$\tau \ddot{\theta}_3 + \dot{\theta}_3 + k\theta_3 = a J \sin \omega t + \frac{aG}{2} \sin 2\omega t - \frac{aF}{2} \cos 2\omega t + \frac{aF}{2} \quad (\text{A-16})$$

The solution of equation (A-16) is of the form

$$\theta_3 = L \sin \omega t + M \cos \omega t + N \sin 2\omega t + O \cos 2\omega t + P \quad (\text{A-17})$$

where

$$P = \frac{ab(k - \tau\omega^2)}{2k[\omega^2 + (k - \tau\omega^2)]^2} \quad (\text{A-18})$$

The solution of equations (A-9) to (A-10) may be obtained in a similar manner. For a, b, and e of the same order of magnitude and much less than unity,* each successive term in equation (A-6) grows smaller by a factor of a. If θ_1 is of the order of magnitude of unity, θ_3 would be of the order of magnitude of a and $\theta_{(2m+1)}$ would be of the order of magnitude a^m . For small values of a, b, and e, sufficient accuracy is obtained by taking

$$\theta = \theta_1 + \theta_3 + \theta_{2m} \tag{A-19}$$

The value of θ_{2m} is obtained by solving equation (A-11). In this equation, $\theta_{(2m-1)}$ approaches zero since its value is of the order of magnitude a^{m-1} smaller than the value of θ_1 .

With $\theta_{(2m-1)}$ equal to zero, equation (A-11) becomes

$$I\ddot{\theta}_{2m} + C\dot{\theta}_{2m} + (K - mLD - mL A \sin \omega t) \theta_{2m} = 0 \tag{A-20}$$

Setting the damping constant $C = 0$ obtains

$$\ddot{\theta}_{2m} + \left(\frac{K - mLD}{I} - \frac{mLA}{I} \sin \omega t \right) \theta_{2m} = 0 \tag{A-21}$$

This is an equation of the Mathieu type. As discussed by the references 7 and 8, the stability of the Mathieu equation depends on the relative values of $\frac{K - mLD}{I}$ and $\frac{mLA}{I}$. Equation (A-21) will generally be stable for

$$\frac{K - mLD}{I} > \frac{mLA}{I} \tag{A-22}$$

*Values of a, b, e for the LIX unit are given in Appendix A of the classified supplement.

Pendulum units used as accelerometers are low pendulosity highly restrained units. The terms mLD and mLA will be of the same order of magnitude and will be much less than K . Equation (A-21) will therefore be stable for the conditions considered here.

The damping term which was set equal to zero for the above analysis will improve stability. Therefore, the value of θ_{2m} will approach zero.

With very little error*

$$\theta = \theta_1 + \theta_3 \quad (A-23)$$

therefore

$$\begin{aligned} \theta = & F \sin \omega t + G \cos \omega t + J + L \sin \omega t + M \cos \omega t \\ & + N \sin 2 \omega t + O \cos 2 \omega t + P \end{aligned} \quad (A-24)$$

The average value of θ is

$$\bar{\theta} \approx J + P = \frac{e}{k} + \frac{ab(k - \tau\omega^2)}{2k \left[\omega^2 + (k - \tau\omega^2)^2 \right]} \quad (A-25)$$

Substituting values for a , b , and e from equation (A-5)

$$\bar{\theta} = \frac{mLE}{(K - mLD)} + \frac{m^2 L^2 (k - \tau\omega^2) AB}{2(K - mLD) \left[\omega^2 + (k - \tau\omega^2)^2 \right] C} \quad (A-26)$$

*The accuracy with which equation (A-23) approximates equation (A-6) for the LIX unit is given in Appendix A of the classified supplement.

With $D = 0$

$$\theta = \frac{mLE}{K} + \frac{(mL)^2 (1 - \mu) AB}{2K^2 \left[\frac{C^2}{KI} \mu + (1 - \mu)^2 \right]} \quad (A-27)$$

where

$$\mu = \frac{\omega^2 I}{K}$$

With $D \neq 0$ at low frequencies

where

$$\omega^2 \ll \frac{K - mL D}{I}$$

and

$$\omega \ll \frac{K - mL D}{C}$$

$$\bar{\theta} \approx \frac{mLE}{K - mL D} + \frac{(mL)^2 AB}{2 (K - mL D)^2} \quad (A-28)$$

If $\frac{mLD}{K} \ll 1$

$$\bar{\theta} = \frac{mL}{K} \left(1 + \frac{mLD}{K} \right) \left[E + \frac{mL AB}{2K} \left(1 + \frac{mLD}{K} \right) \right] \quad (A-29)$$

Neglecting higher order terms

$$K \bar{\theta} \approx mLE \left[1 + \frac{mL AB}{2KE} + \frac{mLD}{K} \right] \quad (A-30)$$

The three terms in the solution are

1) mLE = torque required to react the average value of acceleration along the "X" direction. If the pendulum is used as an accelerometer, this is the only acceleration that should produce a torque. Any other term is an error.

2) $\frac{(mL)^2_{AB}}{2K} = \frac{(mL A_{vib})^2 \sin 2\beta}{4K} = \text{vibropendulum torque.}$ This term results from a torque rectification due to the vibration input.

3) $\frac{(mL)^2_{DE}}{K} = \frac{(mL A_p)^2 \sin 2\alpha}{2K} = \text{cross-coupling torque}$ caused by the "Y" component of acceleration exerting a torque on the pendulum when it is not in its null position.

At high frequencies

where

$$\omega^2 \gg \frac{K - mL D}{I}$$

and

$$\omega \gg \frac{C}{I}$$

$$\bar{\theta} = \frac{mLE}{K - mL D} - \frac{(mL)^2_{AB}}{2(K - mL D) I \omega^2} \tag{A-31}$$

If $\frac{mLD}{K} \ll 1$ neglecting higher order terms, equation (A-31) becomes

$$K \bar{\theta} = mLE + \frac{(mL)^2_{DE}}{K} - \frac{(mL)^2_{AB}}{2 I \omega^2} \tag{A-32}$$

The third term in equation (A-32), the vibropendulum torque, decreases as the pendulum inertia increases and decreases as the square of frequency.

A. 3 PENDULUM SUBJECTED TO A VIBRATION AT AN ANGLE TO THE PENDULUM SENSITIVE AXIS AND ROTATING ACCELERATION VECTOR

The vibration input is

$$\ddot{Y} = A \sin \omega t + B \cos \omega t$$

$$\ddot{X} = D \sin \omega t \tag{A-33}$$

The input is the general case of a vibration at an angle to the pendulum sensitive axis ($B = 0$) and a vibration produced by an acceleration vector rotating about the pendulum pivot ($A = 0, B = D$) as shown in Fig. A-3.

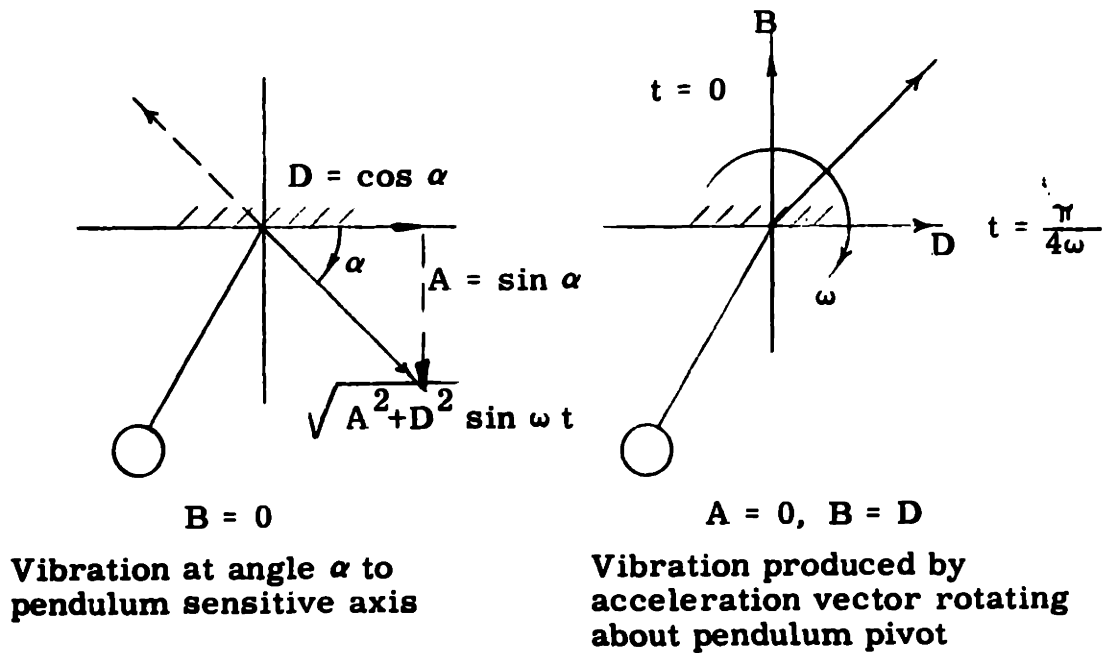


Fig. A-3

For this input equation, (A-1) becomes

$$\tau_1 \ddot{\theta} + \dot{\theta} + (\tau_2 - a \sin \omega t - b \cos \omega t) \theta = d \sin \omega t \tag{A-34}$$

where

$$\begin{aligned} \tau_1 &= \frac{I}{C} & \tau_2 &= \frac{K}{C} & a &= \frac{mLA}{C} \\ b &= \frac{mLB}{C} & d &= \frac{mLD}{C} \end{aligned} \quad (\text{A-35})$$

By the reasoning outlined in Section A. 2, the solution of equation (A-34) is obtained as the series

$$\theta = \theta_1 + \theta_3 + \theta_5 + \dots + \theta_{(2m-1)} + \theta_{2m} \quad (\text{A-6}) \text{ repeated}$$

where

$$\tau_1 \ddot{\theta}_1 + \dot{\theta}_1 + \tau_2 \theta_1 = d \sin \omega t \quad (\text{A-36})$$

$$\tau_1 \ddot{\theta}_3 + \dot{\theta}_3 + \tau_2 \theta_3 = (a \sin \omega t + b \cos \omega t) \theta_1 \quad (\text{A-37})$$

$$\tau_1 \ddot{\theta}_5 + \dot{\theta}_5 + \tau_2 \theta_5 = (a \sin \omega t + b \cos \omega t) \theta_3 \quad (\text{A-38})$$

Consecutively to

$$\tau_1 \ddot{\theta}_{(2m-1)} + \dot{\theta}_{(2m-1)} + \tau_2 \theta_{(2m-1)} = (a \sin \omega t + b \cos \omega t) \theta_{(2m-3)} \quad (\text{A-39})$$

$$\tau_1 \ddot{\theta}_{2m} + \dot{\theta}_{2m} + (\tau_2 - a \sin \omega t - b \cos \omega t) \theta_{2m} = (a \sin \omega t + b \cos \omega t) \theta_{(2m-2)} \quad (\text{A-40})$$

The solution of equation (A-36) is of the form

$$\theta_1 = E \sin \omega t + F \cos \omega t$$

where

$$E = \frac{(\tau_2 - \tau_1 \omega^2) d}{\omega^2 + (\tau_2 - \tau_1 \omega^2)^2} \quad (\text{A-42})$$

The sinusoidal terms will average zero for a vibration period; therefore, the average pendulum deflection ($\bar{\theta}$) is equal to G or

$$\bar{\theta} = \frac{(mL)^2 D \left[(\tau_2 - \tau_1 \omega^2) A - \omega B \right]}{2KC \left[\omega^2 + (\tau_2 - \tau_1 \omega^2)^2 \right]} \quad (A-50)$$

with $B = 0$

$$\bar{\theta} = \frac{(mL)^2 AD (1 - \mu)}{2K^2 \left[\frac{C^2}{KI} \mu + (1 - \mu)^2 \right]} \quad (A-51)$$

where

$$\mu = \frac{\omega^2 I}{K}$$

With $B \neq 0$ at low frequency

where

$$\omega^2 \ll \frac{K}{I}$$

$$\omega \ll \frac{K}{C}$$

and

$$\omega \ll \frac{KA}{CB}$$

$$K\bar{\theta} = \frac{(mL)^2 AD}{2K} \quad (A-52)$$

This is the vibropendulum torque.

At high frequency

where

$$\omega^2 \gg \frac{K}{I}$$

$$\omega \gg \frac{B}{A} \frac{C}{I}$$

and

$$\omega \gg \frac{C}{I}$$

$$K\bar{\theta} = \frac{-(mL)^2 AD}{2I} \left(\frac{1}{\omega^2} \right) \quad (\text{A-53})$$

Vibropendulum torque decreases as the pendulum inertia increases and decreases as the square of frequency.

When

$$A = 0 \text{ for equation (A-50)}$$

This will be the case of a vibration produced by an acceleration vector rotating about the pendulum pivot.

At high frequencies

where

$$\omega^2 \gg \frac{K}{I}$$

and

$$\omega \gg \frac{C}{I}$$

$$K\bar{\theta} = \frac{-(mL)^2 BDC}{2I^2} \left(\frac{1}{\omega^3} \right) \quad (\text{A-54})$$

At low frequencies

where

$$\omega^2 \ll \frac{K}{I}$$

and

$$\omega \ll \frac{K}{C}$$

$$K\bar{\theta} = - \frac{(mL)^2 BDC \omega}{2K^2} \quad (\text{A-55})$$

An equation for the vibropendulum torque (M_{vp}) the torque produced by a vibration ($a \sin \omega t$) at an angle (α) to the pendulum sensitive axis can be obtained from equation (A-26) with $D = E = 0$ or from equation (A-50) with $B = 0$

$$M_{(vp)} = \frac{(mLa)^2 \sin 2\alpha (1 - \mu)}{4K \left[(1 - \mu)^2 + \mu \left(\frac{C^2}{KI} \right) \right]} \quad (\text{A-56})$$

where

$$\mu = \frac{I \omega^2}{K}$$

$\left(M_{(vp)} \right) \frac{4K}{(mLa)^2 \sin 2\alpha}$ has been plotted vs. μ in Fig. 3-6 for various values of $\frac{C^2}{KI}$.

BIBLIOGRAPHY

1. East, George W., Performance of a Pendulous Integrating Gyro Accelerometer Under Environmental Conditions, T-164, Instrumentation Laboratory, Massachusetts Institute of Technology, Cambridge 39, Massachusetts, May 1958 (CONFIDENTIAL).*
2. White, John F., Jr., Errors of Idealized Pendulous Integrating Gyro Accelerometers, T-170, Instrumentation Laboratory, Massachusetts Institute of Technology, Cambridge 39, Massachusetts, June 1958 (CONFIDENTIAL).*
3. Grohe, L. R., Hall, E. J., Sapuppo, M. S., Scoville, A. E., The MIT 25IRIG Inertial Reference Integrating Gyro Unit and the MIT 25PIG Pendulous Integrating Gyro Unit, R-141, Instrumentation Laboratory, Massachusetts Institute of Technology, Cambridge 39, Massachusetts, January 1958 (CONFIDENTIAL).*
4. Rosenes, Oscar, Analysis of Cross-Coupling and Vibration Errors in a PIGA, E-824, Instrumentation Laboratory, Massachusetts Institute of Technology, Cambridge 39, Massachusetts, June 15, 1959.

*None of the above titles are classified; the classification refers to the degree of security handling required of the material in the reports.

- 5. **Rosenes, Oscar, Servo Amplifier for a Pendulous Integrating Gyro Accelerometer, E-814, Instrumentation Laboratory, Massachusetts Institute of Technology, Cambridge 39, Massachusetts, March 15, 1959.**
- 6. **Weinstock, Herbert, A Study of the Response of the Single-Degree-of-Freedom Integrating Gyroscopes to Angular Vibration, E-885,** Instrumentation Laboratory, Massachusetts Institute of Technology, Cambridge 39, Massachusetts, January 1960.**
- 7. **Stoker, J. J., Nonlinear Vibration in Mechanical and Electrical Systems, Interscience Publishing Company, Incorporated, New York, 1950.**
- 8. **Minorsky, N., Introduction to Nonlinear Mechanics, Edwards Brothers, Incorporated, Ann Arbor, Michigan, 1947.**
- 9. **Den Hartog, J. P., Mechanical Vibration, 2nd Edition, McGraw-Hill Book Company, New York, New York, 1940.**
- 10. **Savant, C. J., Jr., Basic Feedback Control System Design, McGraw-Hill Book Company, New York, New York, 1958.**
- 11. **Draper, C. S., Wrigley, W., Lees, S., Inertial Guidance - A Monograph, Instrumentation Laboratory, Massachusetts Institute of Technology, Cambridge 39, Massachusetts, August 1957 (SECRET).***

***None of the above titles are classified; the classification refers to the degree of security handling required of the material in the reports.**
****Internal distribution only, distributed by permission of Group Leader only.**

12. Denhard, W. G. , Acceleration Information Sheet, LIX Nominal Values, GT-100-LIX**, Inertial Gyro Group, Instrumentation Laboratory, Massachusetts Institute of Technology, Cambridge 39, Massachusetts, July 1960.
13. Denhard, W. G. , Freeman, A. P. , Palmer, P. J. , Gyro Information Sheet 10³PFBG Nominal Values, GT-100-10³PFBG**, Inertial Gyro Group, Instrumentation Laboratory, Massachusetts Institute of Technology, Cambridge 39, Massachusetts, May 1960.
14. Whitman, H. R. , Wales, R. L. , Anderson, J. P. , The Type H, Computing and Accelerometer Unit, R-17, Instrumentation Laboratory, Massachusetts Institute of Technology, Cambridge 39, Massachusetts, September 1953.
15. Haff, W. B. , Meltzer, M. , Effects of Angular Vibration on the Performance of a Single-Degree-of-Freedom Integrating Gyroscope, T-257, Instrumentation Laboratory, Massachusetts Institute of Technology, Cambridge 39, Massachusetts, May 1960.
16. Fellows, W. E. , Vibration Effects on Gyroscopes and Accelerations, Minneapolis-Honeywell Regulator Company, MH Aero Document R-ED 29004-1A, November 1958.

****Internal distribution only, distribution by permission of Group Leader only.**